CHALMERS
UNIVERSITY OF TECHNOLOGY

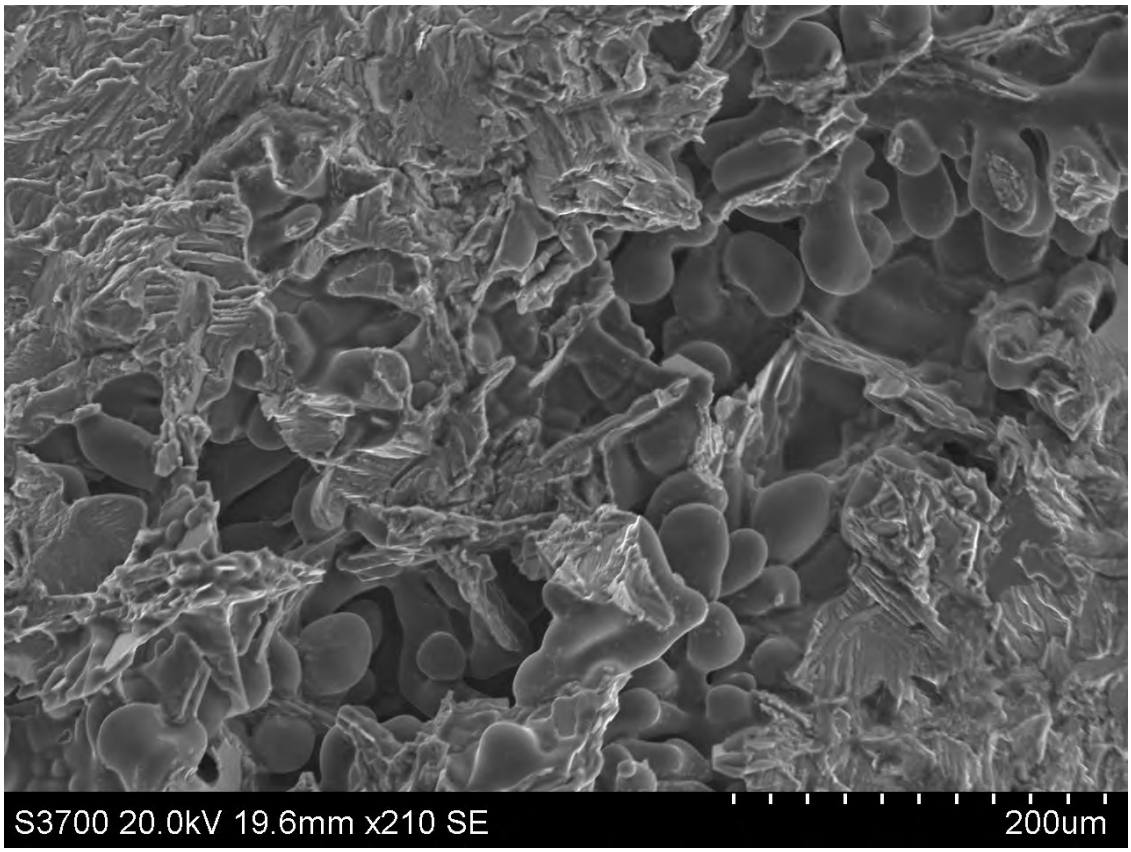

Relationship between Fatigue Properties and Surface Treatment of Aluminum Alloy

Master's Thesis in Materials Science and Technology

UMAIR ALI KHAN

SOROOSH ZAHEDI

DEPARTMENT of INDUSTRIAL and MATERIALS SCIENCE
CHALMERS UNIVERSITY OF TECHNOLOGY
Gothenburg, Sweden 2023
www.chalmers.se

Master's thesis 2023

Relationship between Fatigue Properties and Surface Treatment of Aluminum Alloy

UMAIR ALI KHAN
SOROOSH ZAHEDI

CHALMERS
UNIVERSITY OF TECHNOLOGY

Department of Industrial and Materials Science
Chalmers University of Technology
Gothenburg, Sweden 2023

Relationship between Fatigue Properties and Surface Treatment of Aluminum Alloy

UMAIR ALI KHAN

SOROOSH ZAHEDI

Supervisor: Viktor Räftegård, Volvo Penta
Supervisor: Anton Hvitt Hultmark, Volvo GTT
Examiner: Johan Ahlström, Department of Industrial and Materials Science

Master's Thesis 2023

Chalmers University of Technology
SE-412 96 Gothenburg
Telephone +46 31 772 1000

Cover: SEM image of a PMC sample

Typeset in LaTeX
Printed by Chalmers Reproservice
Gothenburg, Sweden 2023

Relationship between Fatigue Properties and Surface Treatment of Aluminum Alloy
UMAIR ALI KHAN
SOROOSH ZAHEDI
Department of Industrial and Materials Science
Chalmers University of Technology

Abstract

Corrosion has posed a significant challenge within the maritime sector for numerous years. In the 21st century, bolstering the corrosion resistance of alloys, particularly aluminum alloys, has become paramount. Aluminum alloys find widespread use in propulsion systems, boat hulls, and cargo vessels. However, their response to varying water and atmospheric conditions can differ [1]. Different techniques, such as Surface Acid Anodization (SAA) and Chromic Acid Anodization (CAA), are employed to enhance alloy corrosion resistance. Nonetheless, research indicates that anodization can lead to a reduction in fatigue strength of up to 30%.
This master's thesis seeks to examine the effectiveness of three distinct aluminum alloys, each produced through different manufacturing methods, using fatigue testing before and after anodization. The aluminum variants under scrutiny include EN AC-43100 aluminum cast in a permanent mold, AC-43400 produced via high-pressure die-casting, and 6014 sheet metal. The testing employed dog bone samples with a servo fatigue test rig, utilizing the staircase fatigue method. The study also delved into crack formation and microstructural characteristics of cross-sections to investigate failure modes. The results of this investigation aim to lay the groundwork for enhancing fatigue resistance in marine applications of aluminum alloys while minimizing the potential loss of mechanical properties.

Keywords: Corrosion resistance, Fatigue, Aluminium alloys, HPDC, PMC, Sheet Metal, Anodization Molding, Casting.

Acknowledgements

Our master's thesis with Volvo Penta was a challenging journey over 20 weeks. We faced ups and downs but remained determined to achieve our goals. We're grateful for the guidance and support from everyone who helped us explore surface treated alloys. This experience taught us the value of teamwork and the importance of patience. Special thanks to Henrik and Viktor at Volvo Penta, Professor Johan Ahlström, and Elanghovan for their contributions. Lastly, I, Umair, want to express my gratitude to my family for their unwavering support during my academic journey.

UMAIR and SOROOSH,
Gothenburg, September 2023

List of Acronyms

Below is the list of acronyms that have been used throughout this thesis listed in alphabetical order:

ASTM	American Society for Testing and Materials
CAA	Chromic Acid Anodizing
CAP	Chromic Acid Passivation
CCC	Chromatic Conversion Coating
CYC	Cycles
DBS	Dog Bone Specimen
DF	Die cast as Fabricated
DPT	Dye Penetrant Test
HCF	High Cycle Fatigue
HPDC	High Pressure Die Cast
LCF	Low Cycle Fatigue
NDT	Non-Destructive Test
OM	Optical Microscopy
PMC	Permanent Mold Cast
RTS	Residual Tensile Stress
RQ	Research Question
SCM	Stair-Case Method
SEM	Scanning Electron Microscope
SAA	Sulfuric Acid Anodizing
SM	Sheet Metal
ST	Surface Treatment
STR	Servo Test Rig

Nomenclature

Parameters

σ	Stress
σ_m	Mean stress
σ_a	Stress amplitude
E	Young's modulus
N_f	Number of cycles to failure
b	Fatigue strength exponent
c	Ductility exponent in fatigue
ε	Strain
ε_p	Plastic component of strain
ε'_f	Ductility coefficient

Contents

List of Figures

List of Tables

1

Introduction

1.1 Background

It is commonly held that Anodization leads to a decrease in fatigue strength properties by as much as 30 %, prompting the question of its underlying cause[1]. Research indicates that the primary culprit responsible for this reduction in strength is the Pickling process, which precedes Anodization and serves to eliminate impurities, oxides, and scale buildup from the metal that might interfere with subsequent surface treatments. It is important to note that these findings are contingent upon specific test and material conditions, and there exists a dearth of data concerning cast aluminum. For this master's thesis, the alloys chosen from Volvo Penta are High-Pressure Die Cast (EN AC-43400), Permanent Mould Cast (EN AC-43100), and Sheet Metal (6014).The table 1.1 provides the compositional analysis performed at Volvo Powertrain AB at Skövde.

Table 1.1: The chemical analysis from Volvo Powertrain AB, Skövde (wt%)

X	Si	Cu	Mg	Fe	Mn	Zn	Ti	Sr	Cr	Pb
EN AC-43400	8.3	0.11	0.38	0.67	0.11	0.03	0.04	<0.002	<0.01	<0.01
EN AC-43100	10.0	<0.01	0.37	0.15	0.18	0.03	0.07	<0.002	<0.01	<0.01
6014	0.57	0.72	0.22	0.07	0.01	0.03	<0.001	0.01	<0.01	<0.01

Based on the information at hand the following research question was formulated;

1.1.1 Research Question(s) (RQ)

Research Question: What is impact of the anodization process on the fatigue properties of aluminum alloys, specifically High-Pressure Die Cast, Permanent Mold Cast, and Sheet Metal alloys?

Secondary Question: A secondary question that was answered during the thesis was; if strength reduction is observed within any or all of these material groups, is this reduction predominantly influenced by the pickling procedure? Additionally, an ancillary query arises: could a similar procedural step in chemical passivization techniques, such as de-oxidation, yield a comparable effect?

1.2 Objective

The overarching objective of this master's thesis was to execute High Cycle Fatigue pulsating tension tests, reaching a benchmark of 500,000 cycles. For each material type, a minimum of seven samples (if time allowed) underwent fatigue testing both prior to and following anodization, in addition to pickling and de-oxidation as part of the passivization process. These tests were conducted in strict accordance with the standards outlined by ASTM. By employing the staircase method and juxtaposing fatigue cycles of anodized samples against reference samples at their respective force levels, this study aimed to furnish substantiating or contradictory evidence concerning the conjecture that anodization exerts an impact on the material's fatigue longevity. The applied testing matrix is illustrated in Table 1.2, with priorities designated as 1, 2, or 3 – where 1 signifies the highest priority and 3 corresponds to the lowest.

Table 1.2: The Test Matrix

	Untreated	Pickled	Anodized	Priority
PMC	6		5	3
HPDC	7		11	2
SM	8	7	9	1

1.3 Problem Description

The purpose of this thesis was to investigate the fatigue behavior and properties of a test sample before and after anodization. The study began with a literature review and analysis of previous related articles. The high cycle fatigue testing method was used with the study region focused on the thinner area of the test samples. Each test had to achieve a minimum of 500,000 cycles to be eligible for passing the high cycle fatigue criteria set for this thesis. The results of all the tests provided sufficient data to determine how the fatigue properties behaved before and after the applied surface treatment. Failure analysis was then conducted, including OM, SEM, and NDT, to identify and characterize the failure modes. The parameters studied during the fatigue testing are as follows:

- Load
- Fatigue cycle number

For the material characteristic and failure analysis, the following were studied:

1. Interior Defects
2. Crack initiation
3. Oxide film inclusions, Precipitation
4. Surface defects

1.4 Limitations

- The testing area was in the middle of the DBS, which is thinner, and some samples broke within the clamping section or outside of the testing area, rendering them useless for future study.
- The servo test rig (STR) was shared with another group of master students, which limited our access.
- Due to its relatively low hardness, aluminum is categorized as a soft material. This is further compounded by the brittle nature of the incorporated cast alloys and their coarse microstructure containing brittle intermetallics within a soft aluminum matrix. As a result, failures that transpired prior to 500,000 cycles were marked by a uniform crack formation, notably evident in the High-Pressure Die Cast (HPDC) samples. This intricate fracture topography posed difficulties in pinpointing the site of crack initiation and discerning any striations under scanning electron microscopy (SEM). Consequently, the potential insights we could draw from our investigation were constrained, aligning with the challenges posed by the brittle properties of the cast alloys.
  Conversely, in the case of sheet alloys, the reasons for their formidable fractographic complexity remain unclear. This aspect warrants further examination to comprehend why these specific samples presented such intricate fractographic characteristics.
- The fatigue test results could not be accurately predicted beforehand, and some tests lasted for up to three days.
- The servo test rig had to be calibrated periodically, which consumed time and rendered some tests ineligible for the study.
- There were a number of third-party vendors involved with the preparation and surface treatment of the test samples. Lag time at the vendor's end could not be controlled.

2

Theory

2.1 Material Production

2.1.1 High Pressure Die Cast, HPDC (EN AC-43400)

A Cold Chamber process is recommended for the casting of aluminum alloy (EN AC-43400), which contains copper and magnesium. This is especially relevant for high-pressure die casting due to the alloy composition's high melting points and corrosive nature, as indicated by previous research [3]. In the Cold Chamber process, the molten metal is retained in a furnace situated outside the casting machine. It is subsequently introduced into the shot chamber and then injected into the die using a hydraulic piston under high pressure. This casting method proves advantageous for aluminum alloys due to its ability to prevent premature solidification and the potential blockage of the system, issues that can arise with the use of a hot injection system.

It is noteworthy that aluminum alloys suitable for high-pressure die casting (HPDC) often possess distinct properties. For instance, these alloys are typically non-heat-treatable due to certain compositional aspects [3]. Moreover, they commonly feature high alloying content, which contributes to specific mechanical properties and behaviors during the casting process. One crucial factor to consider is the rapid solidification that takes place during HPDC, resulting in a casting skin with distinct properties compared to the bulk material. This rapid solidification can significantly influence fatigue properties, a critical consideration.

Furthermore, the presence of gas porosity is another aspect that can be characteristic of HPDC aluminum components. This phenomenon is attributed to the rapid cooling and solidification process, potentially affecting the material's structural integrity.

The die base must be strong enough to support the die against the heavy locking pressure applied to it, and often, mechanisms of racks, plates, and pinions are used for pulling cores and ejecting the casting. Ejector pins are used in the ejector half of many dies and actuate after the die opens to push the casting out of the cavity and off any fixed cores. See figure 2.1

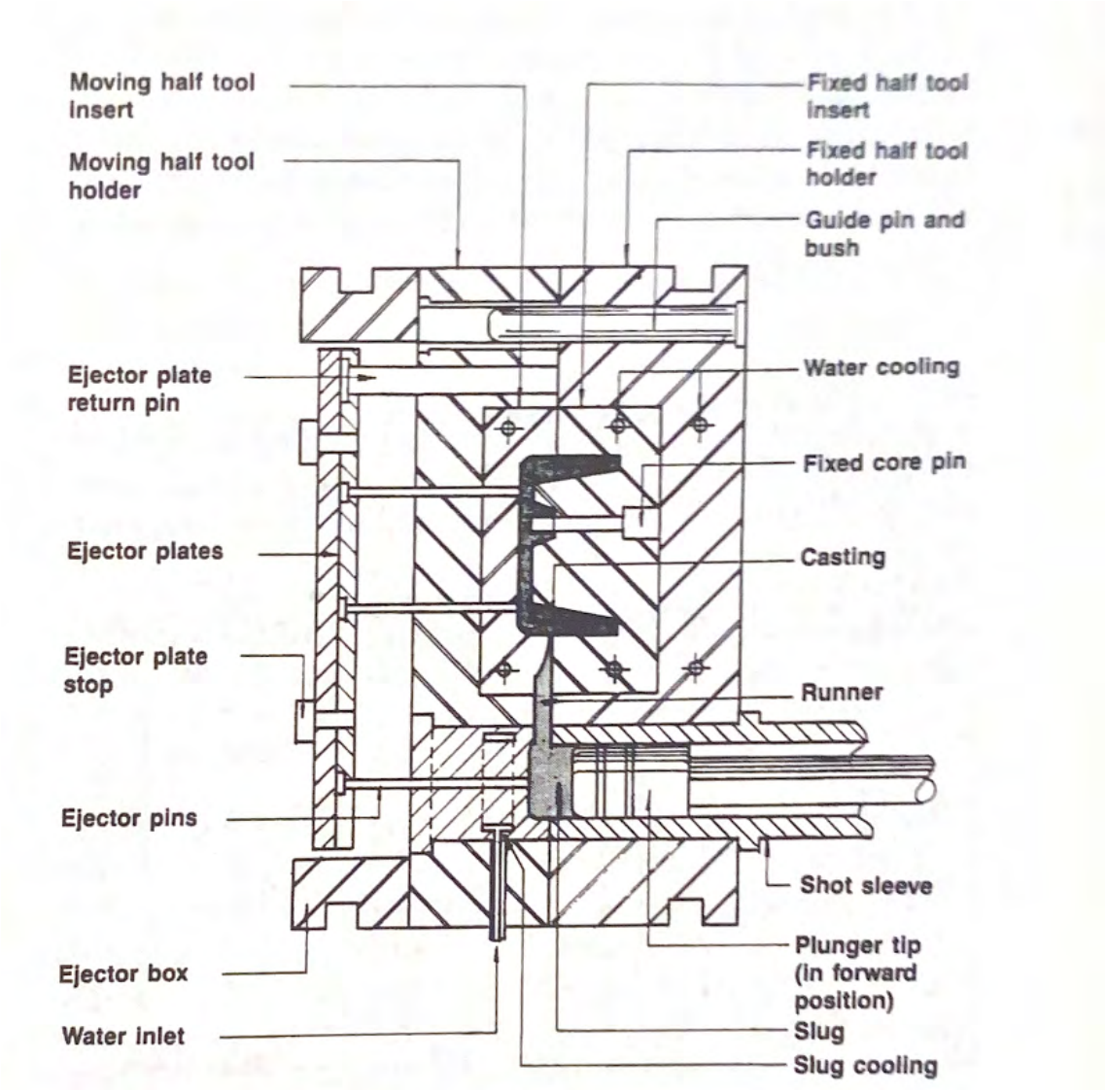

Figure 2.1: HPDC Cold Chamber
Drawing used with permission of the North American Die Casting Association[4].

2.1.2 Permanent Mould Cast, PMC (EN AC-43100)

EN AC-43100 is selected as the designated material for utilization in the Permanent Mold Casting (PMC) process. This choice is driven by the process's ability to achieve enhanced mechanical properties, attributed to a comparatively rapid solidification rate. In the PMC technique, molds made from high-alloy iron or steel are employed. This process entails the pouring of molten metal into permanent metal molds, facilitated either through gravity or under conditions of a low-pressure vacuum. For further clarity, please refer to Figure 2.2. It's important to note that while the solidification rate in PMC is higher compared to traditional sand casting, it is lower when contrasted with High-Pressure Die Casting (HPDC). The favorable attributes often associated with PMC, in contrast to HPDC, can be primarily attributed to the diminished presence of defects, the potential for heat treatment ability, and the utilization of purer alloys featuring reduced iron (Fe) content. This

divergent Fe content is particularly relevant in the context of HPDC, where higher Fe content is necessary to prevent issues like die soldering. The steps for producing part with PMC method are:

1. Spray release agents onto preheated mold surfaces at temperatures between 121-260°C.
2. Close the mold.
3. Heat the alloy to its melting temperature.
4. Pour the molten alloy into the mold.
5. Allow the alloy to solidify.
6. Open the mold.
7. Remove the finished part.

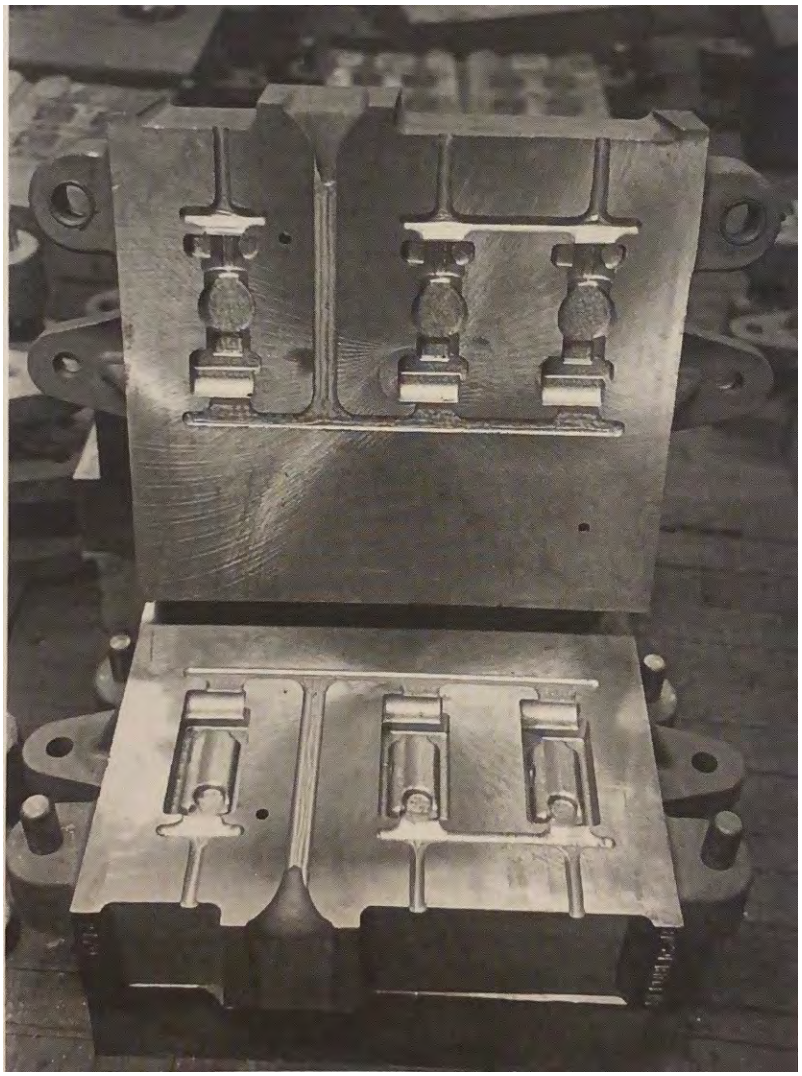

Figure 2.2: PMC Mold
Figure was originally published in the AFS publication "Aluminum Casting Technology," 2nd edition, (Fig. 7-1). Reprinted with permission from the American Foundry Society, Inc., Schaumburg, Illinois, USA (www.afsinc.org) (September, 2023)[4]

2.1.3 Sheet Metal, SM (6014)

According to the ASM Handbook Volume 2A [7], the predominant methods for manufacturing 6014 sheet metal are Twin-roll, refer figure 2.3, strip casting and Twin-belt slab casting, refer figure 2.4.

2.1.4 Twin-Roll Strip

The manufacturing process of producing aluminum sheets through molten metal solidified between moving belts or blocks involves the following steps:

1. Melting: The aluminum alloy is melted in a furnace.
2. Introduction of molten metal: The molten metal is introduced through refractory or ceramic feed tips.
3. Casting: The molten metal is solidified between moving belts or blocks, forming a slab of 10 to 45 mm (0.4 to 1.8 in.) thickness.
4. Rolling: The slab is reduced in-line by high-torque, slow-speed rolling mills to produce either hot-band or finish-gage sheets.
5. Cooling: Cooling is accomplished by arrays of cooling-water applicators and removal devices located on the reverse sides of each belt or block.
6. Cutting: The sheet is cut to a desired length.
7. Finishing: The sheet is cleaned and coated or painted as needed.

The slab casters demonstrate production rates an order of magnitude greater (180,000 Tonnes/yr, or 400 million lb/yr) than strip casters and are relatively alloy-tolerant. The casting speeds of slab casters approximately 4 m/min (13 ft/min). The metallurgical structure of the slab and the re-roll gauge product is similar to that of metal produced from the hot rolling of the conventionally cast ingot.

The twin-belt system employs tension and elaborate guide and support rolls to maintain flatness and minimize distortion. The twin-belt caster can produce at production rates up to 300,000 Tonnes/yr (660 million lb/yr) at a width of 2032 mm (80 in.). Casting speeds can reach 10 m/min (32.8 ft/min).

The twin-block caster employs interlocking precision-machined blocks that form the rolling surfaces. The blocks are water-cooled and dried during the cycle time so that blocks are not in contact with the slab. However, molten aluminum may penetrate the seams formed by adjacent blocks, and while penetration is limited, sheet cosmetics after rolling are affected.

The strip cast stock produced by twin-roll strip casting is the principal source of aluminum foil. The average annual capacity of a strip caster is approximately 18,000 Mg (40 million lb), and casting speeds range widely but average approximately 2.0 to 2.5 m/min (7 to 8 ft/min). The conventional re-roll gauge's of the strip are between 3.18 to 11.4 mm (0.125 to 0.450 in.), which typically serve as stock for subsequent cold rolling or, in some cases, may be rolled in-line to finished sheet gauge's.

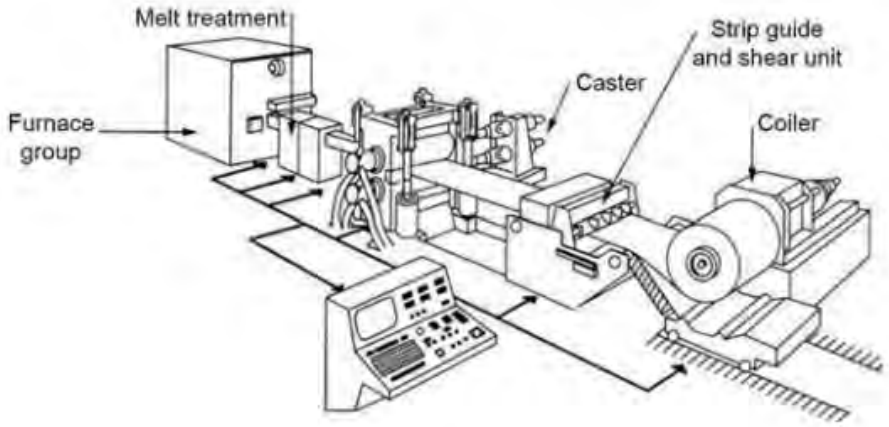

Figure 2.3: Typical arrangement of a twin-roll horizontal caster used in the aluminum industry.[8]

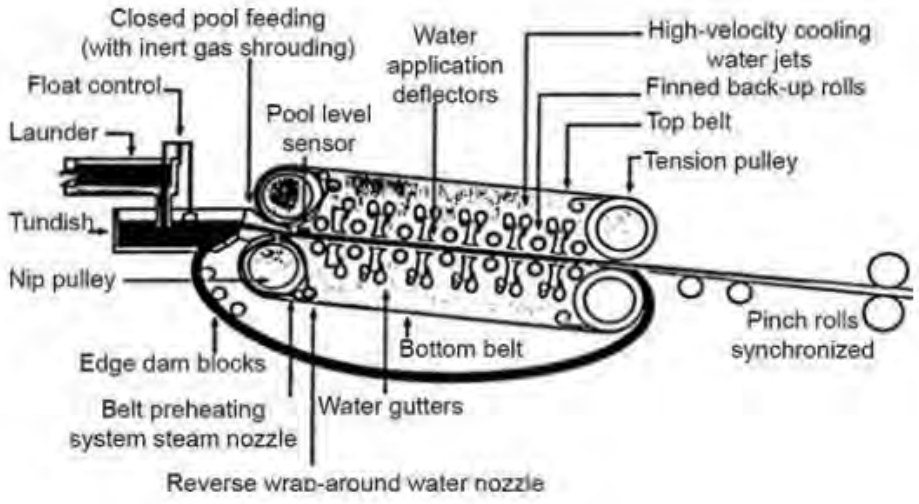

Figure 2.4: Twin-belt slab caster. Courtesy of Light Metal Age. [9]

2.1.5 Surface treatment and Process Overview

Anodization is a crucial surface treatment process widely used in various industries to enhance the properties of metal surfaces. This process involves the formation of a thin, protective oxide layer on the surface of a metal through an electrolytic reaction. The oxide layer provides several key benefits, including improved corrosion resistance and increased surface hardness. In the context of this thesis, Sulphuric Acid Anodization (SAA) was employed as the chosen anodizing method. Specifically, the coating type adhered to the standards outlined in MIL-A-8625F-Type II [5].
Sulphuric Acid Anodization is an electrochemical process that involves immersing the metal workpiece in a bath of sulfuric acid and applying an electrical current. During this process, the metal's surface undergoes a controlled oxidation reaction, resulting in the formation of a stable and protective oxide layer. This layer not only

serves as a barrier against corrosion but also contributes to the overall hardness of the material, making it an attractive choice for various applications.
It's important to note that while Sulphuric Acid Anodization is a well-established method, the specific procedure employed in this thesis may not be widely utilized in industrial practice. Often, anodization practitioners rely on their experience and expertise to fine-tune process parameters to achieve desired results. Factors such as the concentration of the sulfuric acid bath, the applied current, and the duration of the process can all influence the final characteristics of the anodized surface.
One critical aspect of anodization is the determination of coating thickness. In practical applications, ensuring that the oxide layer meets specified thickness requirements is essential. Various methods are employed to gauge coating thickness accurately. Non-Destructive Testing (NDT) techniques, such as eddy current testing or ultrasonic testing, can be used to assess the thickness of the anodized layer without damaging the material. Additionally, a common practice involves analyzing a cross-section of the material under a microscope to precisely measure the thickness of the oxide coating. This quality control step ensures that the anodized components meet the required standards and performance criteria.
In summary, the theory behind anodization, particularly Sulphuric Acid Anodization, is rooted in the electrochemical formation of a protective oxide layer on metal surfaces. The chosen anodization method and adherence to specific standards play a pivotal role in determining the properties of the resulting material. Anodization practitioners rely on both their expertise and specialized testing methods to ensure the quality and performance of anodized components in various applications.

2.2 Fatigue

2.2.1 Elastic Straining- High-Cycle Fatigue

In the traditional approach to fatigue life analysis, fatigue strength is commonly represented by an S-N curve 2.5. This curve illustrates a material's ability to withstand cyclic loading conditions. Under high-cycle fatigue conditions, where the number of cycles to failure (N_f) is relatively large, the fracture response of a material follows the elastic regime. The relationship between stress amplitude (σ_a) and the number of reversals ($2N_f$) is described by the Basquin relationship. It can be expressed as:

$$\sigma_a = \sigma_f (2N_f)^b \tag{2.1}$$

Here, σ_f represents the fatigue strength coefficient, N_f is the number of cycles to failure, and b is the fatigue strength exponent. On a log-log plot, this relationship appears as a straight line with a slope of b. In high-cycle fatigue, the material's behavior is primarily elastic, and the stress amplitude is directly related to the elastic strain amplitude ($\frac{\varepsilon_e}{2}$).

$$\frac{\Delta\varepsilon_e}{2} = \frac{\sigma_a}{E} = \frac{\sigma'_f}{E}(2N_f)^b \tag{2.2}$$

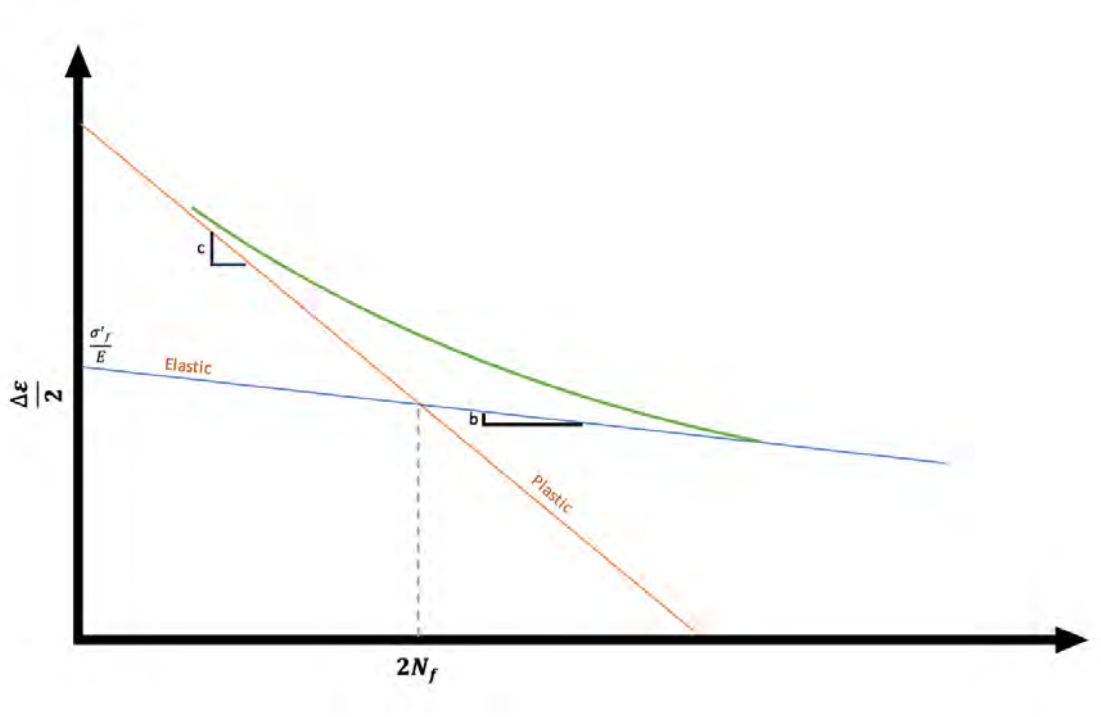

Figure 2.5: Like S-N curve but with logarithmic strain amplitude – proportional to stress amplitude for elastic response

2.2.2 Plastic Straining- Low-cycle Fatigue

Here, $\frac{\varepsilon_p}{2}$ represents the amplitude of plastic strain, ε_f is the ductility coefficient in fatigue, $2N_f$ is the number of reversals to failure, and c is the ductility exponent in fatigue.In the presence of measurable plastic deformation, materials respond differently to strain cycling compared to stress cycling. Under low-cycle fatigue conditions, characterized by a smaller number of cycles to failure, the fracture response involves significant plastic deformation in each cycle. The Manson-Coffin relationship is more suitable for describing the behavior in this regime. It can be expressed as:

$$\frac{\Delta\varepsilon_p}{2} = \varepsilon'_f(2N_f)^c \tag{2.3}$$

On a log-log plot, this relationship appears as a straight line with a slope of c. A smaller value of c indicates a longer fatigue life. In low-cycle fatigue, the material's response is predominantly governed by plastic deformation.

The transition between high-cycle and low-cycle fatigue occurs based on the strain amplitudes experienced by the material. At large total-strain amplitudes, the fatigue life curve tends to follow the plastic curve, while at low total-strain amplitudes, it tends to align with the elastic curve. This behavior is illustrated schematically in figure 2.5. The distinction between the two regimes is important, as high-cycle fatigue primarily involves elastic stresses, while low-cycle fatigue incorporates both

elastic and plastic strains.

$$\frac{\varepsilon_t}{2} = \frac{\varepsilon_e}{2} + \frac{\varepsilon_p}{2} = (\frac{\sigma_f}{E})(2N_f)^b + \varepsilon_f(2N_f)^c \tag{2.4}$$

2.2.3 High Cycle Fatigue Testing Methodology

To achieve high cycle fatigue for each sample, the set-up for tensile fatigue testing involved the use of a servo test rig, STR, and the staircase method, SCM. The test samples were designed to fail within the designated test area during each high cycle fatigue run, however, the test was stopped in case the sample had reached 500,000 cycles, CYC. Following this, Dye penetrant testing, DPT, was applied to detect any cracks or failures.

2.3 Material Characteristic and failure analysis

After conducting the fatigue test, the first step of the experimental procedure was to assign a unique identification number to each sample and take photographs of them for documentation. These photographs were then used in all subsequent phases of the examination process, which included surface treatment, examination of fractured samples, and sectioning the samples for preparation purposes.

2.3.1 Visual Inspection and Documentation

The initial stage of the experimental procedure involved assigning a unique identification number to each sample, capturing images of them for documentation purposes, and utilizing these photographs throughout all phases of the examination process. These steps included surface treatment, examination of fractured samples, and sectioning for sample preparation.

2.3.2 Dye Penetrant Testing

Upon reaching 500,000 cycles, the test samples were replaced with new ones. The non-destructive testing method Dye Penetrant Testing (DPT) method was identified as the most appropriate for detecting surface macro cracks in non-conductive materials such as aluminum.

2.3.3 Light Optical Microscopy

Light optical microscopy (LOM) examination was conducted at the Volvo Material Technology Department using three different microscopes, namely Leica MZFLIII, figure 3.5a,the Leica M205C, figure 2.6b, and Leica DMI5000 M, figure 3.5c. The observations were made at various magnifications. Specifically, Magnifications of 0.8 were employed, with a scale of 2.5 mm for capturing overview images and a scale of 3.2 for pinpointing the approximate crack propagation area. The region of interest was identified for further analysis using scanning electron microscopy.

(a) Leica MZFLIII, **(b)** Leica M205C **(c)** Leica DMI5000 M

Figure 2.6: Microscopes

2.3.4 Sample preparation

In order to utilize the Lecia DM1500 M, sample preparation is essential. This involves molding the sample before it can be analyzed using the equipment. The sample preparation process was carried out by the staff at Volvo Material Technology department.

- **Sectioning**
  After achieving successful results, further research on the grain structure surrounding the crack required proper sectioning. In the figure 2.7, two symbols were used for sectioning: **X** and ↑, which pinpointed the selected areas for the next steps. The **X** symbol was used to indicate a perpendicular direction to the surface, while the ↑ symbol indicated a perpendicular direction to the sectioned area.

Figure 2.7: DF-A-F2 sectioned

- **Cutting :** Prior to cutting aluminum, it is crucial to select a suitable cutting tool, ensure proper feed speed, and use a high-quality cut-off wheel to prevent damage to the material. In this particular case, the Discotom-6 2.8 cutting tool was utilized, and a high-quality num60A25 cut-off wheel was mounted on the machine for cutting the sample. Care was taken to avoid damaging the part during the cutting process.

Figure 2.8: Discotom-6

- **Molding specification:** On the basis of the data provided in Table 2.1, it can be inferred that OP-U suspension is suitable for polishing. To determine the optimal amount of a chemical substance required to achieve a desired concentration in a solution, we utilized M-Mol and M-Chem, considering a particle size of 3 μm.

Table 2.1: Preparation method for Aluminum Silicon Cast [12]

Grinding/Polishing Step		PG	FG	DP	OP
Surface		MD-Molto	MD-Largo	M-Mol	M-Chem
Abrasive	Type	Diamond	Diamond	Diamond	Collodial silica
	Size	# 220	9 μ m	3 μ m	0,04 μ m
Suspention/ Lubricant		Water	150	150	150
RPM		300	Diapro Allegr/Largo 9	DiaPro Mol R3	OP-U Nondry
Force(N)		25	30	30	15
TIME(min)		Unit plane	4	3	1

Due to the variability in the molding materials, we chose Levofast as a non-cast mold as it provided superior resolution compared to the conductive and cast materials when observed under the Leica DMI5000 M and also good for soft material such as aluminum. However, since the selected molding material was not conductive, we utilized conductive tape for further preparation in order to make the samples conductive and perform SEM analysis on them. For instance, copper. The table 2.2 shows the Levofast selection guide

Table 2.2: LevoFast material properties for soft material [13]

Material	Melamine with mineral and glass filler
Type	Thermosetting
Shrinkage,	* (Lowest shrinkage)
Hardness,	*** (softest)
Removal rate	High
Process t	N/A
Quality(ml)	25
Heating t(min.)	3.5
Heating pressure (bar)	250
Cooling time(min.)	2
Cooling rate	High
TPT	5

- **Polishing:** According to the table 2.1 the prepare suspension was OP .Inaditon silicon carbide 220, 500, 1200, 2000 were used respectively to polish the samples Based on the information presented in table 2.1.

2.3.5 SEM

The Scanning Electron Microscope or SEM is a very powerful tool in analyzing topography, composition and microstructure of metals, ceramics and other materials. Samples are prepared by cutting, moulding in a conductive resin, grinding, and polishing the desired surface for inspection. Electron beam produced by heating a tungsten filament that emits electrons is focused on the sample. The beam

is scanned on the surface of the sample in a raster pattern and electrons scattered from the surface are detected using detectors. The brightness and contrast of the images reveals information on the topography, composition and other properties of the fracture surface. Hitachi S-3700N SEM, as seen in figure 2.9, at Volvo Material Technology, was utilized during the thesis to analyze specific locations on different samples. Fatigue striations, which are perpendicular to the direction of crack propagation, and beach marks can also be observed using SEM. Overall, the purpose of utilizing SEM was to detect these features and gain insight into the causes of fatigue failures.

Figure 2.9: Hitachi S-3700N

2.4 Assumptions and propositions

The thesis commences with a review of the relevant literature, which provides evidence that anodization decreases the fatigue life by around 30% [10]. The study demonstrates that the strength of fatigue is directly impacted by anodization due to the hard and brittle nature of anodic coatings. Under mechanical loading, cracks will propagate in both thin and thick coatings. In the case of Sulphuric Acid Anodization (SAA), the crack originates in the anodized film and grows and penetrates into the substrate. However, it was noteworthy that most of the literature sources do not highlight strength reduction for cast aluminium.

2.5 Concepts and constructs

During a period of 20 weeks, the aim was to comprehensively investigate and delineate the effects of Sulphuric Acid Anodization, SAA, pickling and trivalent chrome passivisation on the alloys selected by Volvo Penta for bench marking purposes. The primary objective was to establish with certainty that surface treatment, ST, within these materials is not the root cause of fatigue failure. The ultimate goal of the research was to provide evidence in support of the proposition that SAA is a more dependable method for surface treatment, primarily due to its superior corrosion resistance and hardness properties.

2.6 Relationships and predictions

The experimentation process involved adherence to the test matrix, with subsequent successful testing occurring in the dog bone specimen, DBS, testing area. Any samples that passed the test required analysis to determine the root cause of failure. To discern whether the failure occurred due to anodization or other factors, material characteristic and failure analysis procedures were implemented.

3
Methods

3.1 Outline

The thesis was facilitated by Volvo Penta, Volvo GTT Materials Technology and Chalmers University of Technology. Fatigue testing was carried out at the University, however rest of the equipment and resources were made available by Volvo Penta and Volvo MT.
This chapter offers a comprehensive description of the manufacturing process of the dog bone specimen, including the parameters based on ASTM standards, the material composition, and the process followed for each step. The fatigue testing method, servo test rig setup, and mounting process of the test specimens are also illustrated. Methodology for the light optical microscopy, LOM, and scanning electron microscopy, SEM, analysis is also explained.
Furthermore, this chapter also provides a detailed account of the surface treatment process and the location where it was conducted. The anodized samples were tested once again at Chalmers and data were collected.
Additionally, this chapter sheds light on the material characteristics and failure analysis, including specimen preparation, non destructive testing, NDT, optical microscopy, OM, and scanning electron microscopy, SEM analyses for eligible test samples, thus providing insights for further study.

(a) HPDC-EN AC-43400 **(b)** SM 6014 **(c)** PMC EN AC-43100

Figure 3.1: Test Samples

3.2 Dog Bone Specimen (DBS)

3.2.1 Dog Bone Specimen, DBS, for Fatigue Testing

The primary objective of the fatigue test was to utilize DBS that adheres to the standardized ASTM [2] dimensions, wherein the width and length of all specimens are uniform. Figure 3.2 shows the draft of the DBS and the dimension. However,

the thickness varies depending on the type of alloy. Volvo Penta provided high pressure die cast, HPDC, samples, which were categorized into three batches: Good, Medium, and Bad, based on the surface defects visible to the naked eye. The Good category is comprised of samples with minimal surface defects, while the medium category includes samples with defects outside the testing area used for fatigue tests. Similarly, the samples with the most visible defects were categorized as bad. Additionally, Volvo Penta provided permanent mould cast, PMC, plates, which were cut using a band saw at the Volvo Materials Technology workshop and then sent to Ljungs Mekaniska AB for machining into dog bone specimens (DBS) test samples. Furthermore, the sheet metal, SM, plates provided by Volvo Penta were water-cut at Chalmers Prototype lab.

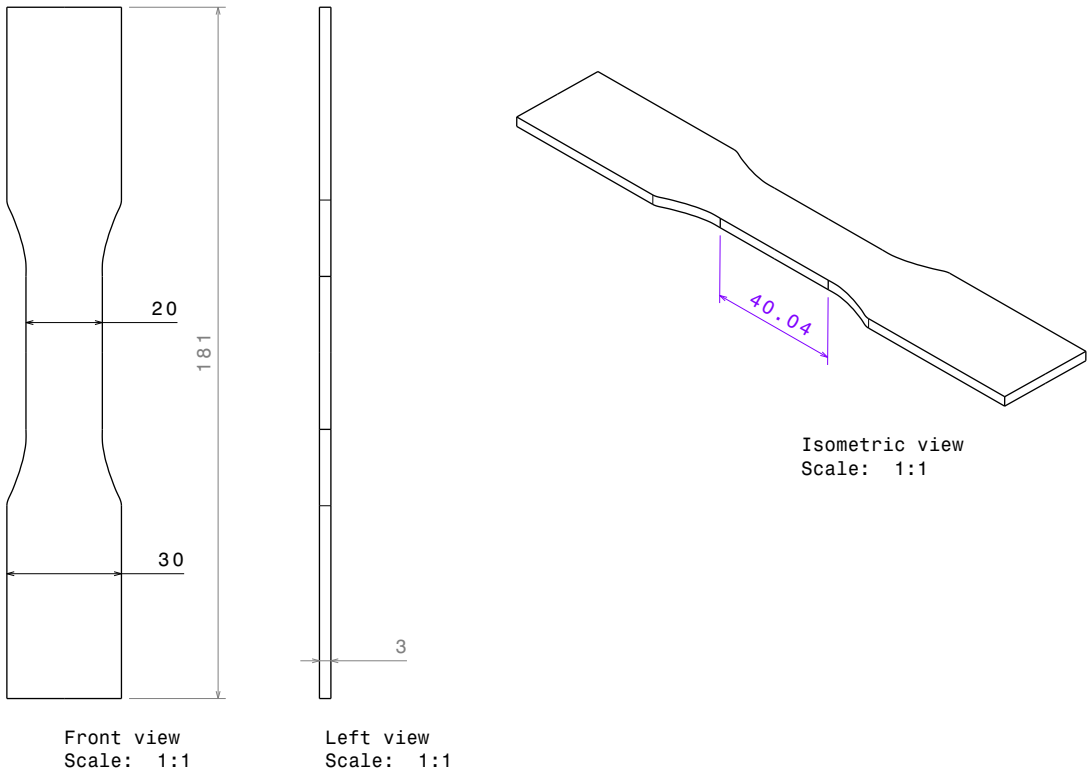

Figure 3.2: Dog Bone fatigue Specimen test sample dimensions (mm)

3.2.2 Dog Bone Specimen, DBS, for Tensile Testing

The Tensile tests were carried out at the Material Technology department of Volvo. As per the ASTM standard [14] for tensile testing, the dimensions differed from those of the fatigue specimens as shown in figure 3.3 . Consequently, the SM tensile DBS were water cut at Chalmers University of Technology's Porto type lab, while the PMC was sent to Ljungs Mekaniska AB for machining, as shown in the figure 3.4 .

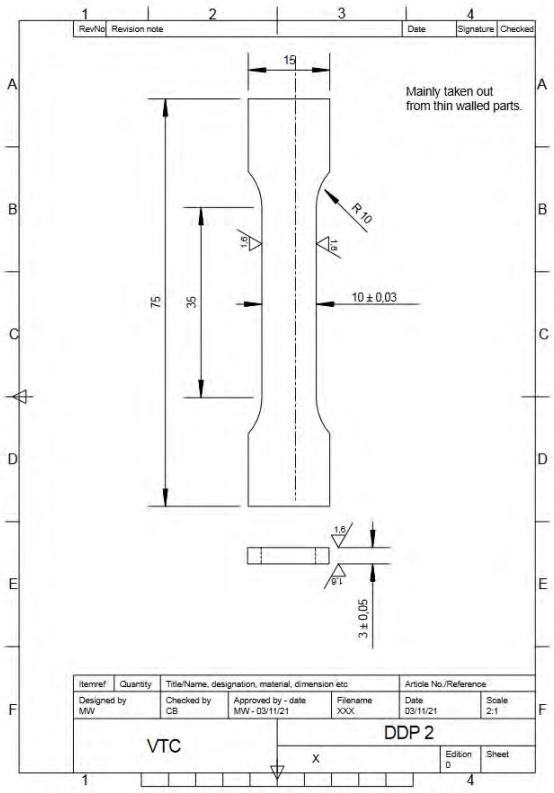

Figure 3.3: Dog Bone tensile Specimen test sample dimensions (mm)

(a) High Pressure Die Cast

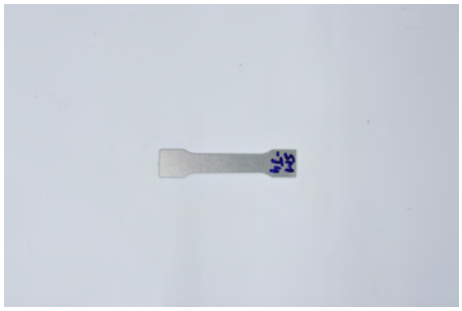

(b) Sheet Metal

(c) Permanent Mold Cast

Figure 3.4: Tensile DBS

3.3 Specimen Preparation

The fractured samples were moulded, ground and polished for investigation under the optical microscope and/or the SEM. The resin used for the mould was non-conductive, however, conductive tape was used when the sample pucks were examined in the SEM. Fractured DBS surfaces were also examined in the SEM. Conductive tape was not applied to these surfaces.

Volvo Penta provided three distinct aluminum alloys with varying elemental compositions. The composition analysis for these alloys is presented in Table 1.1. Each alloy was manufactured differently and procured from a different supplier. This subsection provides detailed information about the suppliers and mechanical properties of each alloy.

3.3.1 Permanent Mould Cast, PMC

Tables presenting the mechanical properties, permanent mold cast PMC, and casting characteristics of test coupons were included in accordance with European casting standards. These test coupons were produced through gravity die casting of PMC plates by Vertech in China. Further details regarding the PMC and casting characteristics and Mechanical properties are available in Table 3.1 and 3.2.

Table 3.1: Casting characteristics [15]

Solidification range °C	Casting temperature °C	Fluidity	Hot tearing resistance	Shrinkage (%)	Pressure tightness
600-550	650-700	Excellent	Excellent	0.5-0.8	Good

Table 3.2: Mechanical properties of PMC [15]

Temper designation	Tensile strength R_m, MPA,min	Yield strength , $R_{P^{0.2}}$, MPA,%, min	Elongation A_{50},%, min	Brinell hardness HB,min
F (as cast)	240	140	1	70

The Volvo materials technology machine shop band saw was used to split the PMC plates into $\approx 190 \times 40$mm pieces. The resulting pieces were sent to Ljungs Mekansika AB for further machining into standard DBS for fatigue testing and surface treatment.

3.3.2 Sheet Metal, SM

The 25 mm sheet metals plates were provided by Volvo Penta which were originally acquired through Volvo Penta According the European standard of manufacturing process [16] for 25 mm Alumiunum sheet metal with thickness of 25 mm the mechanical properties provided in the table below:

Table 3.3: Mechanical properties of Sheet Metal [15]

Temper	Tensile strength R_m MPA	Yield strength, $R_{P^{0.2}}$, MPA,	Elongation at break ,%, min (A_{80})	Uniform Elongation $Ag(\%)$	Plastic Strain Ratio	Strain Hardening Exponent
T4-T4P	195-260	95-135	≥ 23	≥ 19	≥ 0.6	≥ 0.24

3.3.3 High Pressure Die Cast, HPDC

The HPDCs components were supplied to Volvo Penta by one of its vendors. However, there was notable variability in the manufacturing quality of these HPDCs. According to references such as "Fundamentals of Aluminium Metallurgy" [17], HPDCs often exhibit defects, including micro vortices, shrinkage porosity, and gas porosity, which were indeed observed in our collected samples. To ensure consistency, a meticulous sorting process was conducted on a total of 100 samples, leading to the selection of a batch with the least defects. This chosen batch of non-anodized HPDCs became part of the study.
Interestingly, anodized HPDCs, obtained from a prior project through Provexa, were also part of the study. These anodized HPDCs underwent a similar sorting procedure to maintain a standardized approach.
It is relevant to note that both anodized and non-anodized HPDC samples, including those from the same batch, were obtained from a vendor not previously known to us through Jönköping University. Additionally, certain samples were anodized by Provexa, although they were not utilized in the original thesis work they were intended for.

3.3.4 Surface Treatment (Anodization)

Anodization is a process that creates a thin protective oxide layer on a metal surface using an electrolytic reaction, improving corrosion resistance and hardness. Sulphuric Acid Anodization (SAA) was used in this thesis, with the coating type chosen from MIL-A-8625F-Type II [5].
It's worth noting that, as mentioned, this specific procedure is not commonly employed. In practice, anodized often rely on their experience to determine appropriate process parameters. Additionally, coating thickness can typically be gauged using methods such as Non-Destructive Testing (NDT) or by analyzing a cross-section of the material under a microscope.

3.4 Tensile Testing Result

The objective of the tensile test was to determine the yield strength/force of each type of specimen. The results of the tensile test are depicted in the figure 3.5. Since the stair-case method was employed during the fatigue testing process (as described in section 3.5), the data obtained from the tensile test provided a general estimation of the maximum force applied during the fatigue test.

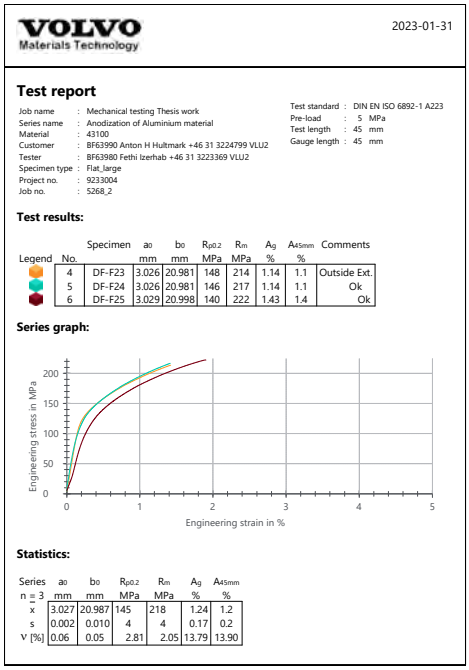

VOLVO Materials Technology

2023-01-31

Test report

Job name : Mechanical testing Thesis work
Series name : Anodization of Aluminium material
Material : 43100
Customer : BF63990 Anton H Hultmark +46 31 3224799 VLU2
Tester : BF63980 Fethi Izerhab +46 31 3223369 VLU2
Specimen type : Flat_large
Project no. : 9233004
Job no. : 5268_2

Test standard : DIN EN ISO 6892-1 A223
Pre-load : 5 MPa
Test length : 45 mm
Gauge length : 45 mm

Test results:

Legend	No.	Specimen	a_0 mm	b_0 mm	$R_{p0.2}$ MPa	R_m MPa	A_g %	A_{45mm} %	Comments
	4	DF-F23	3.026	20.981	148	214	1.14	1.1	Outside Ext.
	5	DF-F24	3.026	20.981	146	217	1.14	1.1	Ok
	6	DF-F25	3.029	20.998	140	222	1.43	1.4	Ok

Series graph:

Statistics:

Series n = 3	a_0 mm	b_0 mm	$R_{p0.2}$ MPa	R_m MPa	A_g %	A_{45mm} %
$\bar{x}$	3.027	20.987	145	218	1.24	1.2
s	0.002	0.010	4	4	0.17	0.2
v [%]	0.06	0.05	2.81	2.05	13.79	13.90

5268_2.zs2 **Page 1/1**

(a) HPDC-EN AC-43400

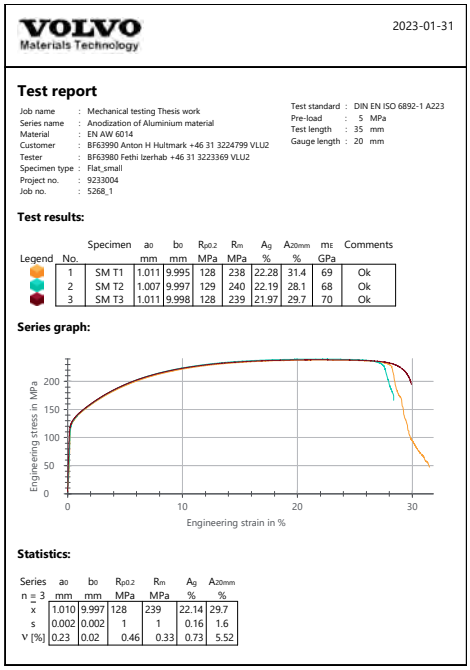

VOLVO Materials Technology

2023-01-31

Test report

Job name : Mechanical testing Thesis work
Series name : Anodization of Aluminium material
Material : EN AW 6014
Customer : BF63990 Anton H Hultmark +46 31 3224799 VLU2
Tester : BF63980 Fethi Izerhab +46 31 3223369 VLU2
Specimen type : Flat_small
Project no. : 9233004
Job no. : 5268_1

Test standard : DIN EN ISO 6892-1 A223
Pre-load : 5 MPa
Test length : 35 mm
Gauge length : 20 mm

Test results:

Legend	No.	Specimen	a_0 mm	b_0 mm	$R_{p0.2}$ MPa	R_m MPa	A_g %	A_{20mm} %	m_E GPa	Comments
	1	SM T1	1.011	9.995	128	238	22.28	31.4	69	Ok
	2	SM T2	1.007	9.997	129	240	22.19	28.1	68	Ok
	3	SM T3	1.011	9.998	128	239	21.97	29.7	70	Ok

Series graph:

Statistics:

Series n = 3	a_0 mm	b_0 mm	$R_{p0.2}$ MPa	R_m MPa	A_g %	A_{20mm} %
$\bar{x}$	1.010	9.997	128	239	22.14	29.7
s	0.002	0.002	1	1	0.16	1.6
v [%]	0.23	0.02	0.46	0.33	0.73	5.52

5268_1.zs2 **Page 1/1**

(b) SM 6014

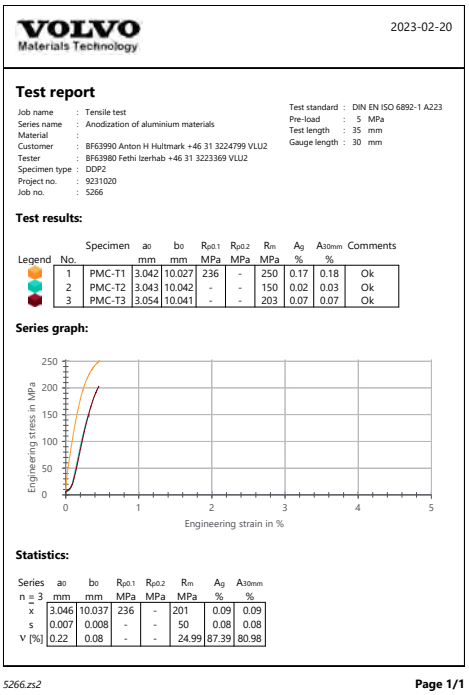

VOLVO Materials Technology

2023-02-20

Test report

Job name : Tensile test
Series name : Anodization of aluminium materials
Material :
Customer : BF63990 Anton H Hultmark +46 31 3224799 VLU2
Tester : BF63980 Fethi Izerhab +46 31 3223369 VLU2
Specimen type : DDP2
Project no. : 9231020
Job no. : 5266

Test standard : DIN EN ISO 6892-1 A223
Pre-load : 5 MPa
Test length : 35 mm
Gauge length : 30 mm

Test results:

Legend	No.	Specimen	a_0 mm	b_0 mm	$R_{p0.1}$ MPa	$R_{p0.2}$ MPa	R_m MPa	A_g %	A_{30mm} %	Comments
	1	PMC-T1	3.042	10.027	236	-	250	0.17	0.18	Ok
	2	PMC-T2	3.043	10.042	-	-	150	0.02	0.03	Ok
	3	PMC-T3	3.054	10.041	-	-	203	0.07	0.07	Ok

Series graph:

Statistics:

Series n = 3	a_0 mm	b_0 mm	$R_{p0.1}$ MPa	$R_{p0.2}$ MPa	R_m MPa	A_g %	A_{30mm} %
$\bar{x}$	3.046	10.037	236	-	201	0.09	0.09
s	0.007	0.008	-	-	50	0.08	0.08
v [%]	0.22	0.08	-	-	24.99	87.39	80.98

5266.zs2 **Page 1/1**

(c) PMC EN AC-43100

Figure 3.5: Tensile Result

3.5 Fatigue Testing

3.5.1 Test Rig Set-up

Fatigue testing was the intended focus of the thesis and was performed on the fatigue rig at Chalmers University of Technology.In practice, this type of testing is used by materials engineers and designers to ensure the durability of the materials and components they use or develop for any specific purpose. It also helps in determining the life span of a product. Fatigue testing is a tool to enhance the safety and longevity of products and designs before they enter the real world. Aluminium alloys after being surface treated develop high corrosion resistance, which is of paramount importance when operating under extreme weather conditions. However, when subjected to cyclic loading and unloading, fatigue is developed in the material causing it to fail during operation. Initially, the untreated samples were tested to acquire a baseline value for the tests for Sheet Metal, High-Pressure die-cast, and Permanent mould-cast samples.

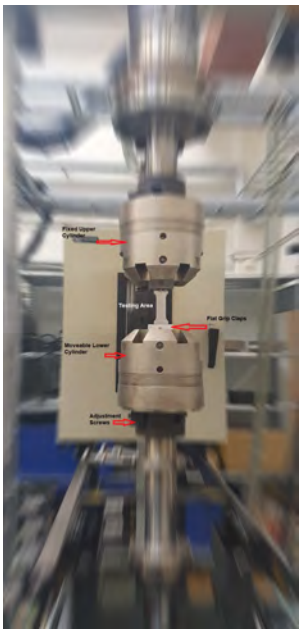

Figure 3.6: Fatigue test rig

Figure 3.6 below shows the Fatigue Test Rig at Chalmers that was used for the entire project. Here it is loaded with one HPDC anodized samples. A threshold of five hundred thousand (500,000) cycles was set to simulate high fatigue life of the test samples.

The flat structure of the samples necessitated the use of flat grip clamps on the test rig. For cylindrical samples, a different set of clamps was employed. The lower cylinder had the capability to move, while the upper cylinder remained stationary. Throughout the testing process, the rig maintained a constant frequency of 20Hz, while the amplitude of the applied load varied based on the material characteristics, following the staircase method.

During the mounting of the samples in the testing area, the clamps were used to secure them. Initially, the lower clamps were tightened, and then the cylinder was raised to ensure that the sample was fully positioned in the upper clamps. The upper clamps were subsequently tightened to the appropriate torque. Proper alignment of both cylinders was ensured to minimize any unwanted vibrations during the testing process. Following each test, the data were recorded, and the number of cycles was compared to the threshold value.

Excessive tightening of the clamps resulted in compression forces at the clamping section, thereby increasing the likelihood of failure within the clamps. To mitigate this, a Torque Wrench with a meter was utilized, set to 20-30 KN.

In relation to Figure 3.7, the first step involved setting a new sample, assigning a name to it, and activating the Stress control feature (Number 1). Figure 3.8 illustrates the stress control section, which includes the selection of a Segment shape, specifically choosing a Sine waveform with a frequency of 20Hz. In the context of the thesis, the focus is on the tensile fatigue test without compression. Consequently,

the absolute pressure for end level two remained consistently at 0, while end level one represented the tensile force.
Ensuring safety is of paramount importance when operating the machine. Hence, it is crucial to perform a double check on the detector, as depicted in Figure 3.9, prior to utilizing the machine. Setting the force and displacement within appropriate limits is also vital. In the event of a failure, when the bottom piston descends beyond the lower limit, the machine automatically shuts off and suspends the process. Additionally, activating the interlock during the clamping of the upper clamp is imperative for safety purposes.
The lower piston, as stated, is capable of vertical movement through manual control, as illustrated in Figure 3.10. Displacement calculations were employed primarily prior to the initiation of the radio system in order to determine an appropriate position. Signal Auto Offset, depicted in Figure 3.11, was utilized to reset the displacement and force values to zero.
Once the top part has been clamped and tighten, the "Enable manual control" option should be unchecked in the manual command window. Subsequently, the process should be locked using the station manager window, followed by clicking on the play symbol to initiate the test.

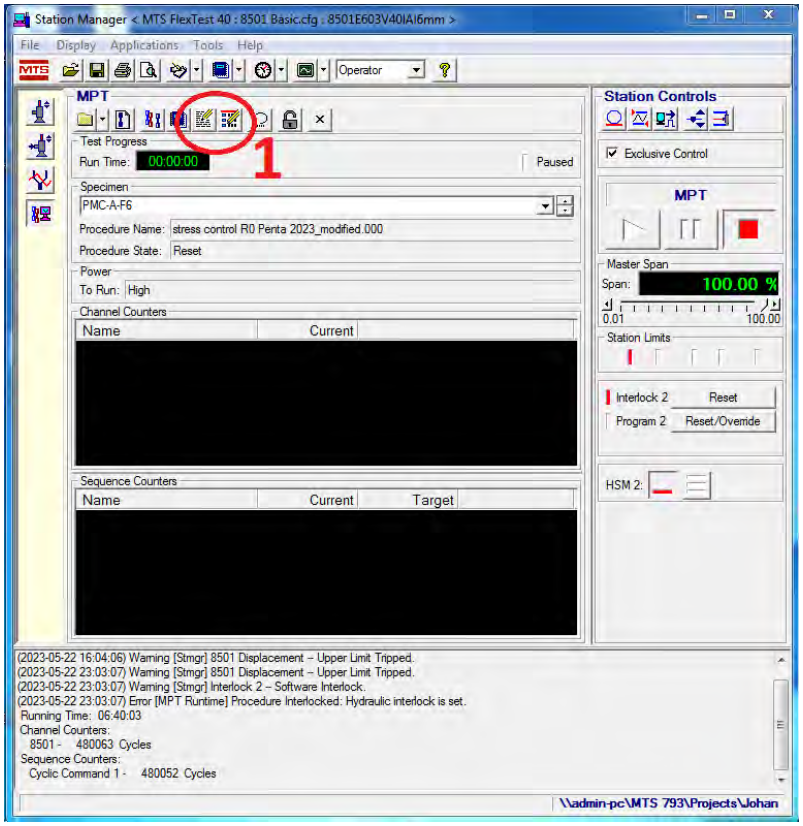

Figure 3.7: Station manager

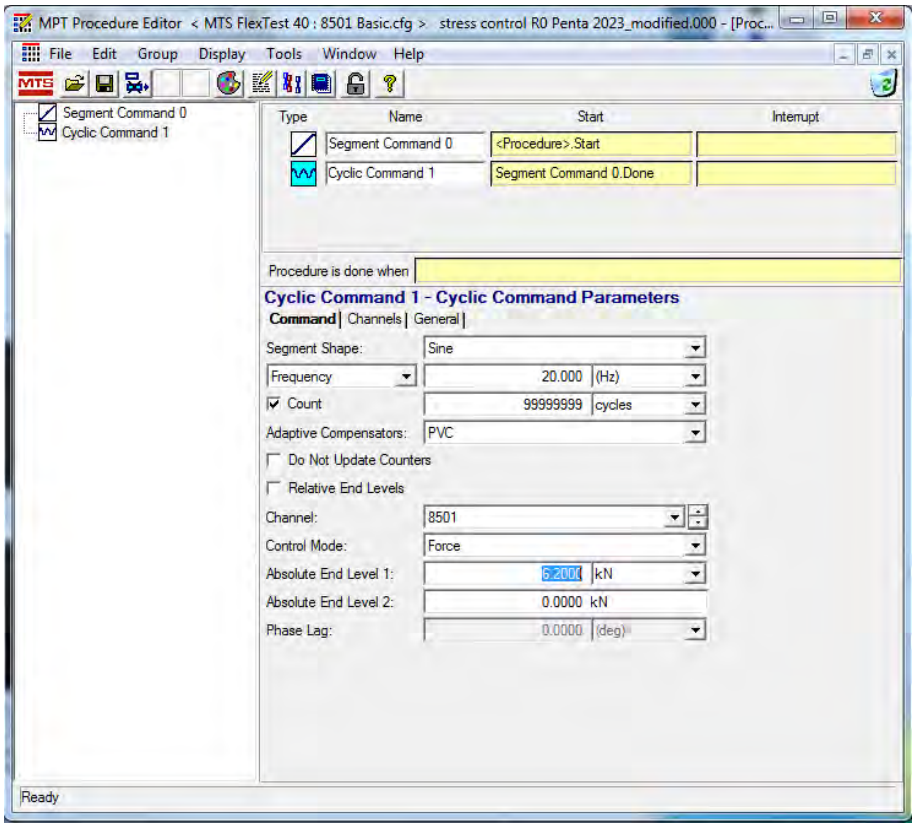

Figure 3.8: Stress control

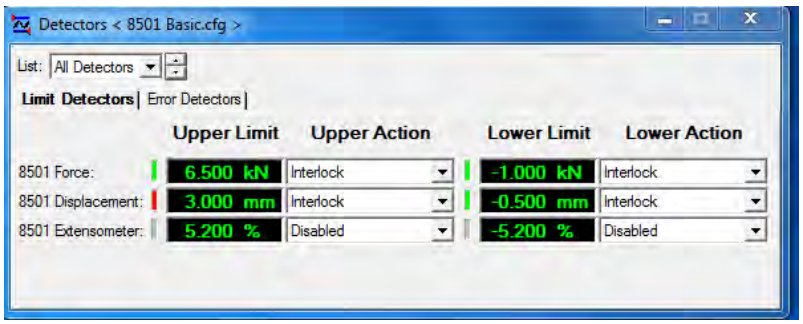

Figure 3.9: Safety detector

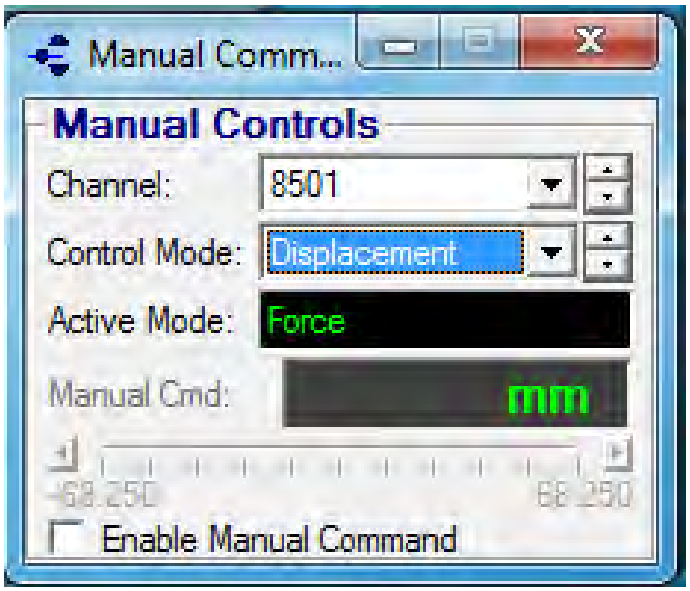

Figure 3.10: Manual control

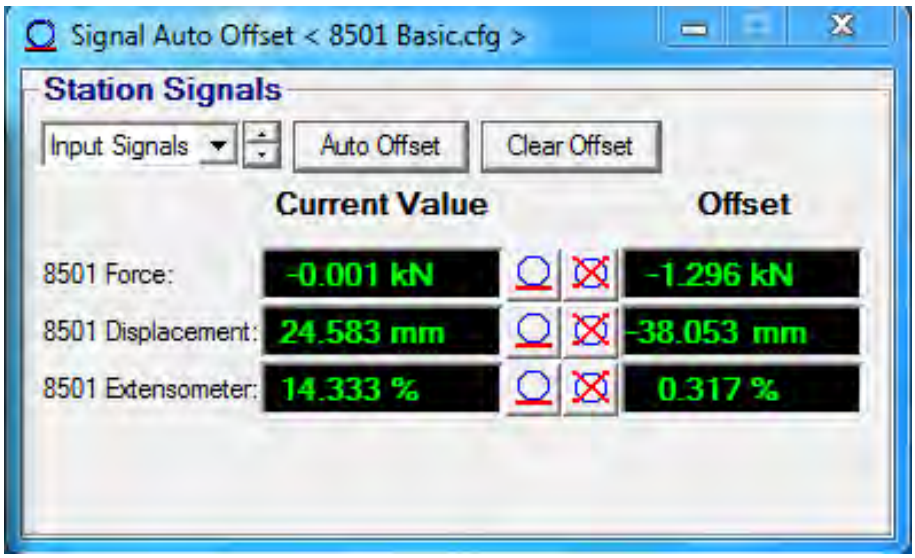

Figure 3.11: Offsets

3.5.2 Stair Case Method

The staircase testing technique serves as a valuable tool in ascertaining the appropriate stress thresholds for different test samples, typically permitting a maximum of 1E7 cycles [11]. Prior to initiating fatigue testing, it is customary to conduct a tensile test on Polymer Matrix Composites (PMC) and Sheet Metal (SM) materials to establish their respective yield stresses. Subsequently, the upper limit of stress for subsequent testing is determined based on these outcomes, with the upper boundary for the staircase method being constrained by the yield stress level.
The application of the staircase method was employed to delineate the limits of high cycle fatigue life for test samples produced via pressure die-cast HPDC, Sheet Metal SM, and Permanent mold-cast PMC techniques. This methodological approach en-

compassed the exposure of the specimens to an incrementally adjusted load or stress level at predetermined intervals, either augmenting or diminishing it systematically. By methodically varying these stress levels, the staircase method facilitated the assessment of fatigue performance and the establishment of the endurance limit for each casting method.

High-Pressure Die Cast (HPDC):
A nominal stress value of 100 MPa was set for testing the HPDC samples. Taking account of the geometry of the sample, the load was calculated to be 6.3 KN. The load was increased or decreased gradually if the sample achieved the threshold or broke well before it respectively. Tables 3.4 and 3.5 show the HPDC test data for reference and anodized samples respectively.

Table 3.4: HPDC Reference

Sample	Force(KN)	Cycles	Stress (MPa)
DF-F15	5.5	90295	87
DF-F9	5.5	106019	87
DF-F8	6	14985	95
DF-F37	6.5	295150	103
DF-F11	7	128262	110
DF-F54	6.5	183709	103
DF-F53	6.2	644145	98

Table 3.5: HPDC Anodized

Sample	Force (KN)	Cycles	Stress (MPa)
DF-A-F3	7	540896	110
DF-A-F5	7	236890	110
DF-A-F4	7	38855	110
DF-A-F8	6.8	63855	108
DF-A-F9	6.8	58719	108
DF-A-F6	6.7	528422	106
DF-A-F7	6.7	65832	106
DF-A-F2	6.5	716252	103
DF-A-F10	6.5	42084	103
DF-A-F13	6.4	529240	101
DF-A-F11	6	386697	95
DF-A-F12	6	54949	95
DF-A-F20	5.8	1440415	92

Sheet Metal (SM):
A nominal stress value of 38 MPa was set for testing the SM samples. Taking account of the geometry of the sample, the load was calculated to be 2.4 KN. The load was increased or decreased gradually if the sample achieved the threshold or broke well before it respectively. Table 3.6, table 3.7 and table 3.8 depict the data for sheet metal reference, anodized and pickled samples respectively.
It is pertinent to mention here that the samples SM-P-F5 and SM-P-F2 did not break.However, sample SM-P-F3 suffered a fatigue fracture after achieving 655179 cycles and was deemed as a successful test run.

Table 3.6: Sheet Metal - Reference

Sample	Force (KN)	Cycles	Stress (MPa)
SM-1	2.5	140877	40
SM-2	2.4	207875	38
SM-3	2.4	206633	38
SM-4	2.4	301076	38
SM-5	2.4	335470	38
SM-6	2.2	520102	35
SM-7	1.7	865364	27
SM-8	1.7	4716865	27

Table 3.7: Sheet Metal Anodized

Sample	Force (KN)	Cycles	Stress (MPa)
SM-A-F1	2.4	90000	38
SM-A-F2	2.4	117242	38
SM-A-F3	2.2	195802	35
SM-A-F7	2.2	150024	35
SM-A-F6	2.0	408399	32
SM-A-F9	2.0	255726	32
SM-A-F5	1.8	431607	29
SM-A-F4	1.7	1077395	27

Table 3.8: Sheet Metal Pickled

Sample	Force (KN)	Cycles	Stress (MPa)
SM-P-F1	2.4	238080	38
SM-P-F4	2.4	353523	38
SM-A-F7	2.3	753262	36
SM-P-F3	2.2	655179	35
SM-P-F6	2.2	1540529	35
SM-P-F5	2.0	1342255	32
SM-P-F2	1.7	4550874	27

,

Permanent Mould Cast (PMC):
Similar to HPDC, nominal stress value of 100 MPa was set for testing the PMC samples as well. Taking account of the geometry of the sample, the load was calculated to be 6.3 KN. The load was gradually increased or decreased if the sample achieved the threshold or broke well before it respectively.
Samples were dismounted when fractured or when reached the 500,000 cyc threshold. The fractured samples were carefully bagged and labeled for further investigation. Tables 3.9 and 3.10 depict the test data results in a tabular form.

Table 3.9: PMC - Reference

Sample	Force (KN)	Cycles	Stress (MPa)
PMC-F1	6.5	327130	101
PMC-F2	6.2	107977	98
PMC-F4	6.2	337227	98
PMC-F6	6	85303	95
PMC-F7	6	1591886	95

Table 3.10: PMC Anodized

Sample	Force (KN)	Cycles	Stress (MPa)
PMC-A-F4	6.5	945898	104
PMC-A-F5	6.5	227223	104
PMC-A-F2	6.2	1100	98
PMC-A-F3	6.2	500990	98
PMC-A-F1	6.4	1148000	101
PMC-A-F6	6	480063	95
PMC-A-F7	6	167593	95
PMC-A-F8	6	1138966	95

3.6 Material Characteristic and Failure Analysis

The fatigue tested DBS test specimens were inspected using the following methods;

1. Visual Inspection
2. Dye Penetrant Test (DPT)
3. Light Optical Microscopy (LOM)
4. Scanning Electron Microscopy (SEM)

3.6.1 Visual inspection

A visual Inspection of test samples is essential to identify any apparent and visible damage or indications of fracture. This inspection aided in ensuring the integrity and reliability of the tested samples, allowing for immediate identification and evaluation of any visible signs of potential failure or structural flaws. Samples which fractured outside the testing area or within the clamping jaws were immediately rendered invalid for further inspection. Test samples with fatigue fractures within the testing area, even if they did not achieve the 500000 cycle mark, were in some cases cut, moulded, ground and polished for further inspection in under the LOM and SEM.

3.6.1.1 High Pressure Die Cast

Two samples are mentioned in figure 3.12a and 3.12b that did not pass the high cycle fatigue threshold, however the test run was valid as the samples fractured within the testing area.

(a) DF-F9

(b) DF-F15

Figure 3.12: HPDC - reference chosen samples

3.6.1.2 High-Pressure Die Cast-Anodized

Similar to the HPDC reference section, two samples for the HPDC anodized batch are shown in figure 3.13. Both test runs were deemed valid, however, a point to note here was that sample 3.13b did not break and the test was stopped after the threshold cycles had been reached.

(a) DF-A-F5

(b) DF-A-F6

Figure 3.13: HPDC Anodized chosen samples

3.6.1.3 Sheet Metal

Following suit, the sheet metal samples were visually inspected as well for any obvious signs of damage and/or clues as to how the fracture may have been initiated. Figure 3.14 shows two samples from the sheet metal reference batch.

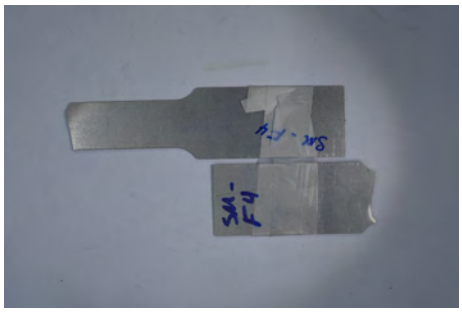

(a) SM-F4

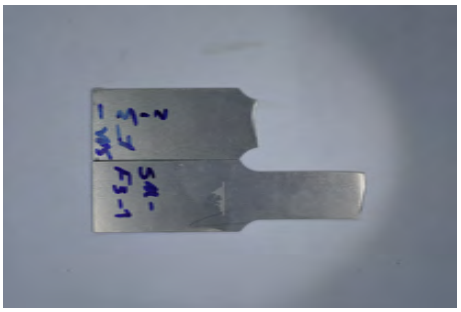

(b) SM-F3

Figure 3.14: SM chosen samples

3.6.1.4 Sheet Metal-Anodized

The sheet metal anodized samples were carefully removed from the test rig for further analysis and two samples are seen in figure 3.15.

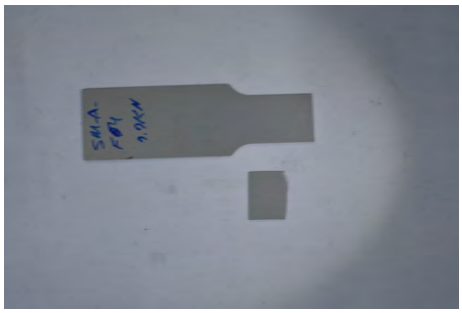

(a) SM-A-F4

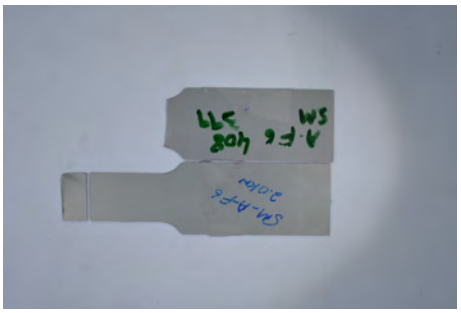

(b) SM-A-F6

Figure 3.15: SM Anodized chosen samples

3.6.1.5 Permanent Mould Cast

The PMC samples were tested in a similar manner on the fatigue rig and data were collected carefully. Figures 3.16 and 4.8b show the reference and anodized samples respectively for the PMC batch that was studied further.

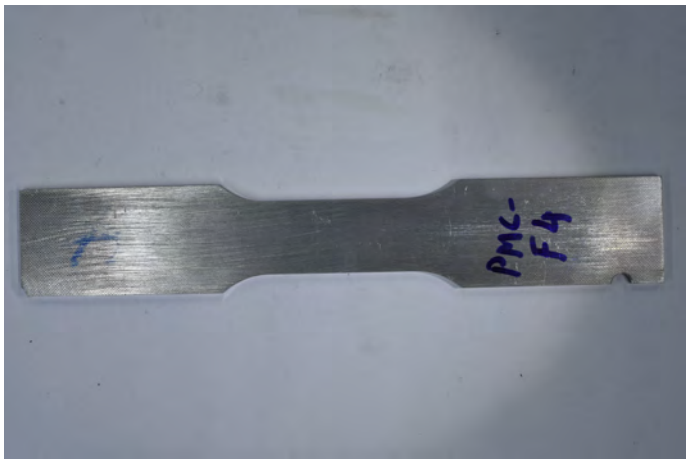

Figure 3.16: PMC-F4

3.6.1.6 Permanent Mould Cast-Anodized

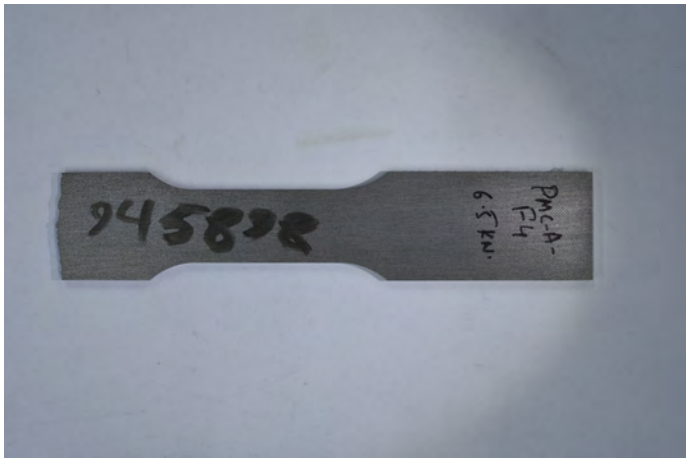

Figure 3.17: PMC-A-F4

3.6.2 Dye Penetrant Test

The dye penetrant test is a crucial inspection method that was employed on the test samples that survived the 500000 cyc threshold and did not break under their respective loads. This test involved applying (spraying) a RED-colored dye on the surface of the sample, allowing it to seep into any surface defects. After a dwell time, the excess dye was removed, and a developer was applied to draw out the dye from the defects. This process was supposed to highlight any surface cracks, porosity, or other discontinuities that might compromise the structural integrity of the aluminum cast.

3.6.3 Light Optical Microscopy

Light Optical Microscopy is a powerful tool for the in-depth study of aluminum alloys where visible bright light and lenses are used to magnify and resolve structures, it allows for detailed examination and analysis of test samples, and aluminum alloy samples for our purposes. Light optical microscopy plays a crucial role in understanding the effects of different alloying elements, heat treatments, and processing techniques on the final material properties, such as strength, corrosion resistance, and mechanical behavior.

4

Results & Discussion

4.1 Data Plots

The test samples were subjected to fatigue testing at Chalmers University of Technology and the data acquired for each batch were plotted as follows,

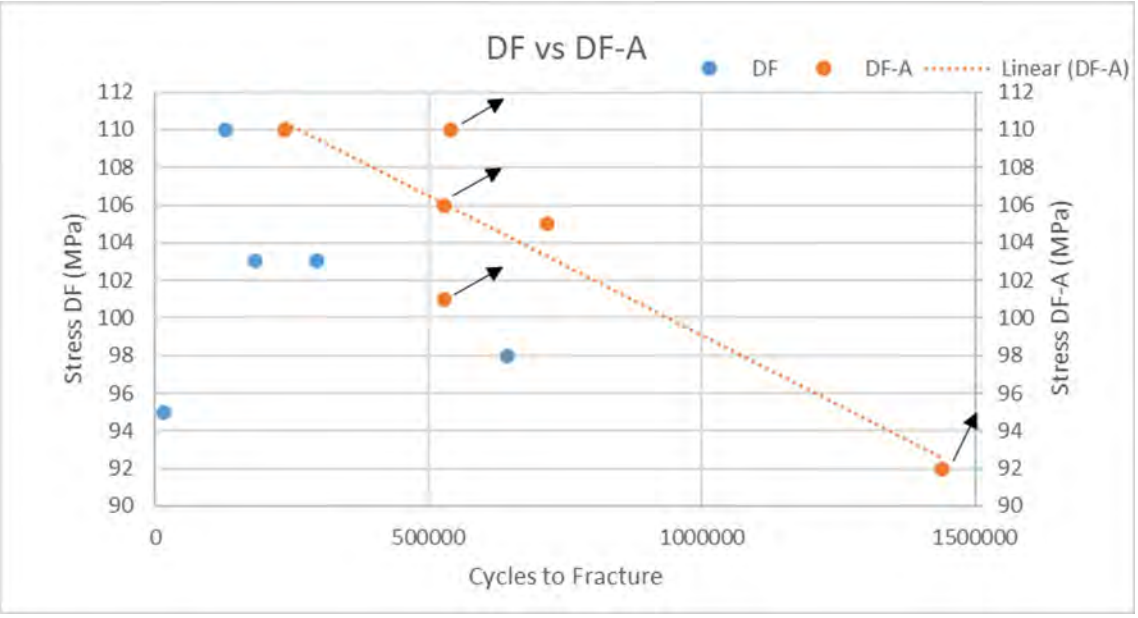

Figure 4.1: Data Plot HPDC

Figure 4.1 shows the data points plotted for the HPDC test samples both before and after amortization along with a trend line for the later batch. The small arrows seen here are the samples that did not break after achieving the threshold value of 500000 cycles. The test was manually stopped for these samples. It is clearly seen that the anodized samples show a higher fatigue strength than the unanodized samples at a prescribed stress level. This trend can also be noted in table 3.4 previously.

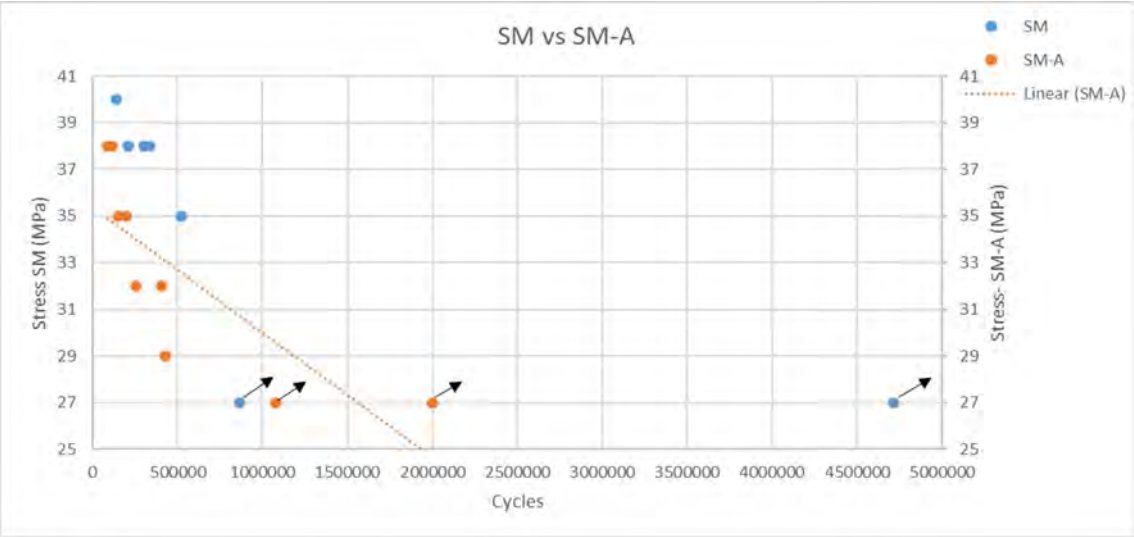

(a) SM vs SM-A

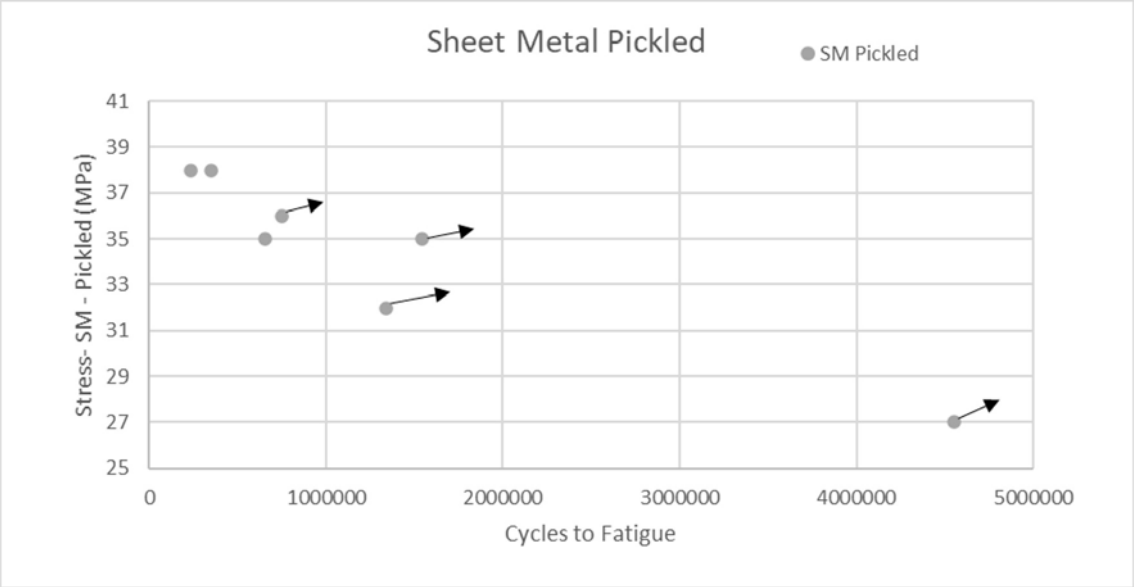

(b) SM Pickled

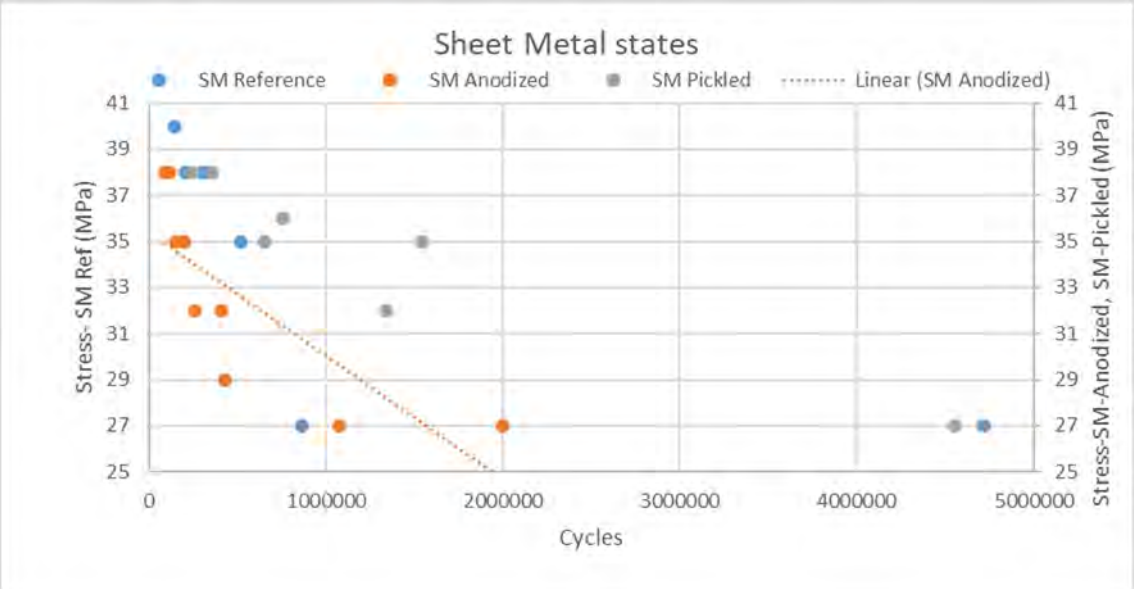

(c) SM 3 States

Figure 4.2: Data Plot Sheet Metal

Figure 4.2 here shows three plots for sheet metal. The first plot 4.2a depicts the comparison of sheet metal samples before and after anodization. Similar to the previous figure, the arrows here also show the samples that did not break and the tests were stopped manually. It is evident that at lower stress levels, the samples showed the best fatigue behavior. Such behavior was expected as the sheet metal displayed the lowest tensile strength out of all the alloys as seen in figure 3.5b. The pickled samples displayed the best fatigue characteristics out of the three states for sheet metal samples. As seen in table 3.8 and figure 4.2b, most of the test runs were successful and had to be manually terminated in order to start a new test. Pickling not only rids the metal of any undesired oxides, or scale build-up but leaves the surface with corrosion pits that prove to be the cause of future fatigue failure. The reason why these test samples behaved the way they did was attributed to the lack of such pits on the surface post-treatment. Once more the arrows point out the samples that did not break. Figure 4.2c shows the comparison of reference, pickled, and anodized sheet metal samples. It is fairly evident that the pickled samples show the best fatigue properties out of the batch staying consistent with the assumption that anodization alone does not cause a decrease in fatigue strength.

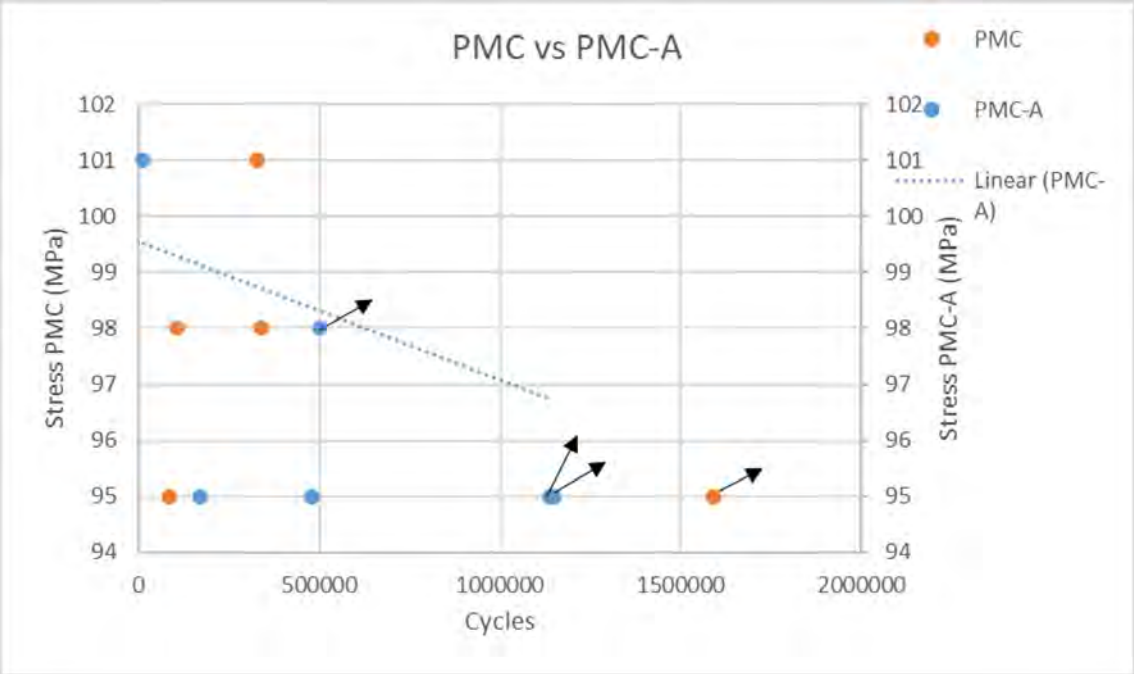

Figure 4.3: Data Plot PMC

Figure 4.3 and tables 3.9 and 3.10 show a spread of data across the various stress levels for permanent mold cast samples. As always the threshold was set at 500000 cycles for a successful high-cycle fatigue run, and the sample had to fracture in the testing area for the test to be valid. The failed samples also display a spread of data owing to the contribution of the presence of pre-solidified material defects, shrinkage porosity, and internal stresses. The in-depth analysis of both the cast materials, i.e. HPDC and PMC, showed a similar pattern of defects causing the samples to fail well before the threshold. Figure 4.4 is an overview of both the cast alloy's anodized

sample. It is seen here that quite a few samples had a successful test run with the HPDC samples having a higher fatigue strength than the PMC samples.

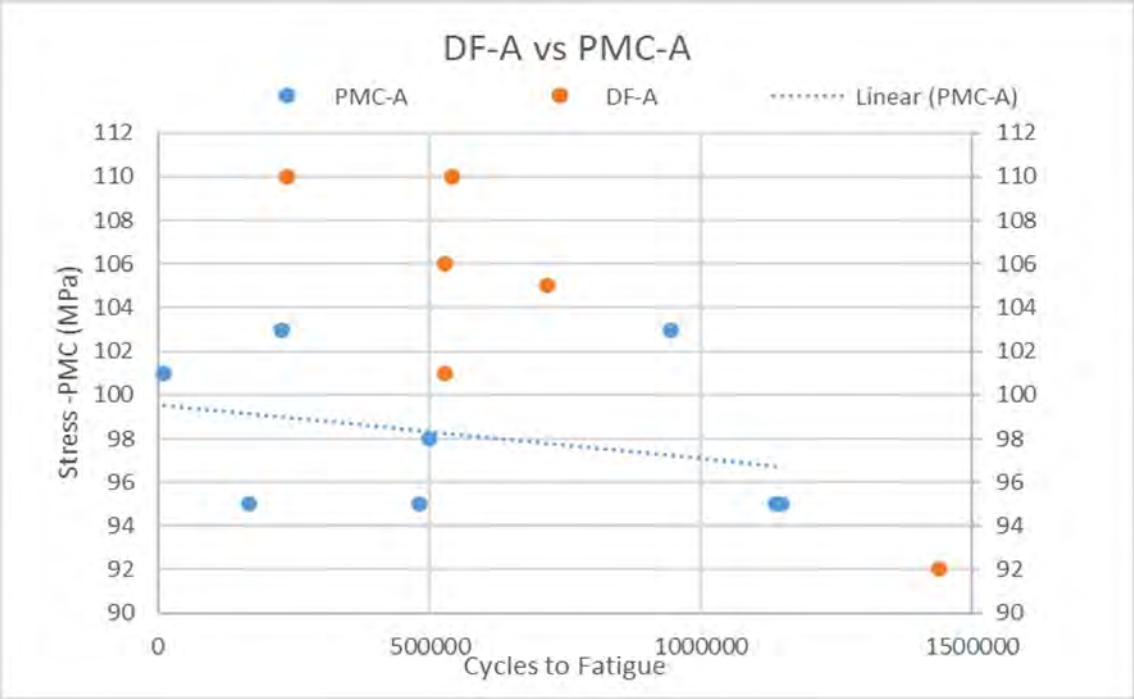

Figure 4.4: Data Plot DFA vs PMCA

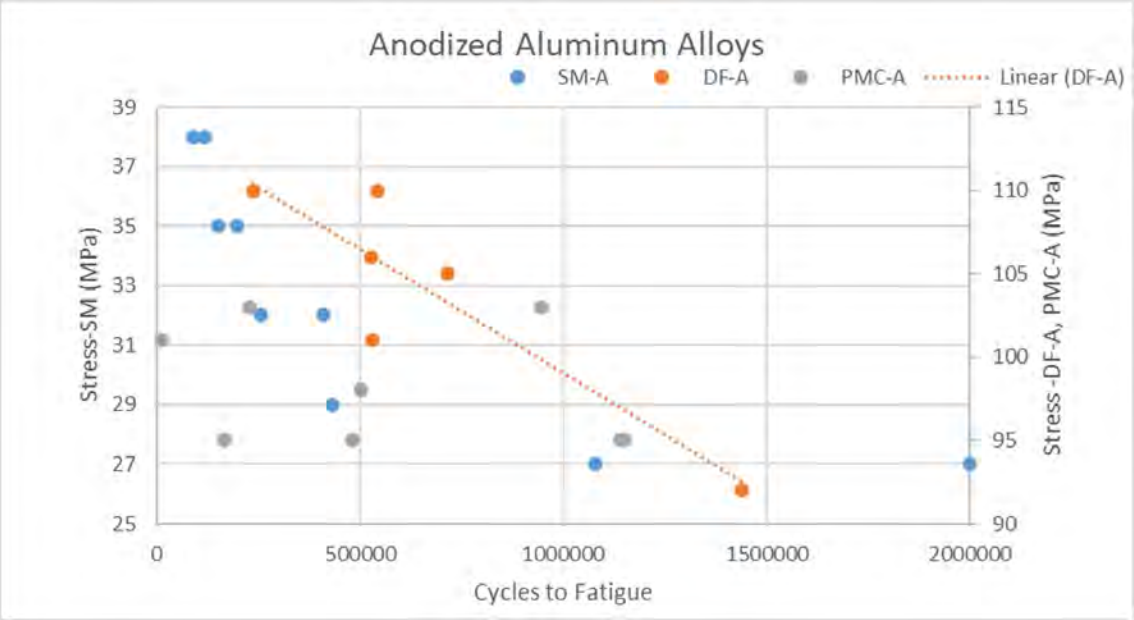

Figure 4.5: Data Plot Anodized Alloys

Fatigue-tested test specimens were subjected to various types of tests including;

1. Visual Inspection
2. Dye Penetrant Test (DPT)
3. Light Optical Microscopy (LOM)
4. Scanning Electron Microscopy (SEM)

4.1.1 Visual Inspection

4.1.1.1 High Pressure Die Cast

Figure 4.6 shows two examples of invalid samples that broke outside the testing area (a & c) and one that did not break at all (b).

(a) DF-A-F4 **(b)** DF-A-F6 **(c)** DF-A-F12

Figure 4.6: DF-A Test Samples

It is evident by looking at figure 4.6a above that the fracture happened outside the testing area specifically in the clamping jaws. Similarly, in figure 4.6c the fracture occurred at the bottom of the sample. Conversely, in figure 4.6b, one sees that the fracture did not initiate. This sample passed the test and survived the threshold. NDT was also performed on 4.6b and no surface cracks were observed.

4.1.1.2 Sheet Metal

Sheet metal samples were visually inspected as well. Figure 4.7 shows how sheet metal samples looked after their respective test runs. One sees that both the un-anodized (reference) and anodized SM samples fractured, however, the pickled sample did not break but showed some signs of physical distortion at the position marked by the arrow. The reference sample fractured very close to the clamping section while still remaining valid. The anodized sample fractured in the middle of the testing region and was also valid. The sample 4.7c showed a rather unusual surface defect post-test. One sees waves, torsion, and buckling effects in the testing area as marked by the arrow. The sample survived 1540529 cycles and did not fracture. The sur-

face defects could be attributed to misalignment of the test top and bottom jaws by applying slight shear along with the designated tension force. Since there was no compression load applied in any of the tests, buckling was ruled out as a possible cause of the defect. The test, however, remains valid.

(a) SM-F3

(b) SM-A-F4

(c) SM-P-F6

Figure 4.7: SM Test Samples

4.1.1.3 Permanent Mould Cast

Similarly, all PMC samples were subjected to visual inspection as well. Samples 4.8a and 4.8b fractured after passing the fatigue test, however, as seen in the respective figures the later one fractured in the clamping area and was deemed as invalid test. On the contrary samples in 4.8c not only survived the high cycle fatigue test but the test had to be manually stopped.

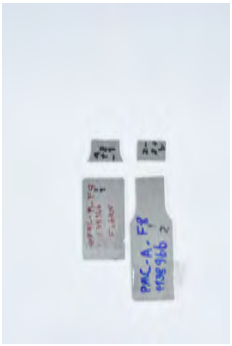

(a) PMC-A-F8

(b) PMC-A-F4

(c) PMC-A-F1 and F3

Figure 4.8: PMC Test Samples

4.1.2 Dye Penetrate Test (DPT)

One unbroken sample from each test batch after the fatigue test was subjected to this NDT test. However, no surface cracks were observed in any of the samples after the developer was applied implying that no surface defects were present.

4.1.3 Light Optical Microscopy (LOM)

The samples were examined under optical microscopes for further analysis and the results are discussed as follows,

4.1.3.1 High Pressure Die Cast

Figure 4.9 shows three spots of concern. Figure 4.10a shows spot 1 zoomed in shows the fracture surface and crack initiation and propagation. Signs of shrinkage are visible close to the surface which leads to further SEM analysis. Figure 4.10b can be taken as a prime example of shrinkage porosity. Figure 4.12 clearly shows the fracture surface and how multiple cracks were initiated at the surface of the sample. Secondary cracks and crack front merger is suspected as well. Cracks are growing into the surface in line with the load direction.
Figures from 4.13 to 4.16 represent the other un-anodized HPDC sample that fractured extremely quickly at a low-stress level. Starting from the left side of the figure 4.16, multiple crack initiation sites along with possible pre-solidified oxide inclusions can be seen before the final static fracture towards the middle and proceeding to the right side.
Figure 4.19 shows the overview of one HPDC anodized sample, while a closeup of the defined sections is shown in the preceding figure 4.20. Just by carefully examining the close-up figure one is able to conclude that the fracture happened near the surface due to the presence of multiple internal defects such as macro-porosities, intermetallics, and possible shrinkage due to solidification.
Figure 4.21 below shows an un-anodized fractured sample. One sees signs of fatigue fracture towards the right end of the figure. The left side of the figure shows a static fracture. Multiple cracks are seen initiating from the surface of the sample and propagating towards the center of the sample. The thick white mark in the center of the figure is suspected to be a double-folded oxide layer, which expedites crack growth by creating internal stresses.

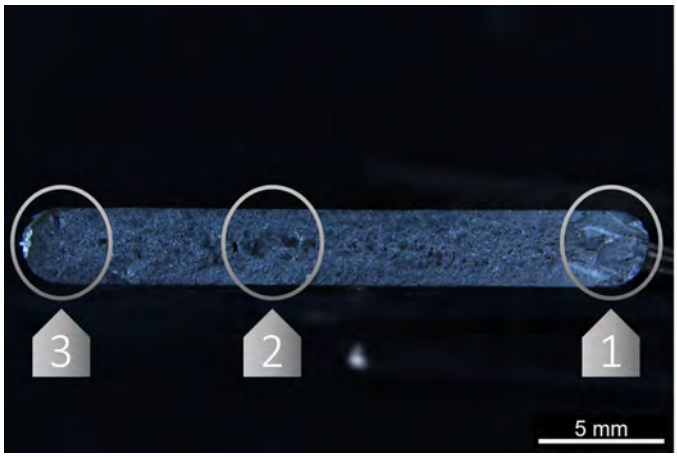

Figure 4.9: DF-F9-1

The three spots marked as 1, 2, and 3 were thought of as probable causes of premature failure in the sample shown in figure 3.12a. A closeup of spot 1 and spot 2 is shown in figure 4.10.

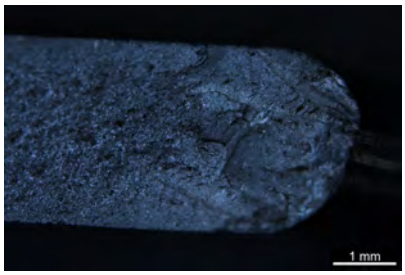

(a) Spot 1

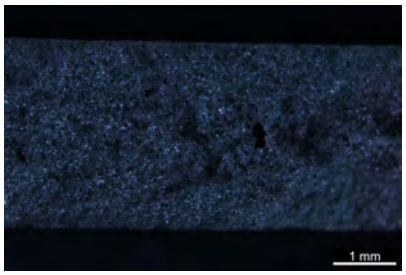

(b) Spot 2

Figure 4.10: DF-F9-1 Defined section

Figure 4.11: DF-F9-2

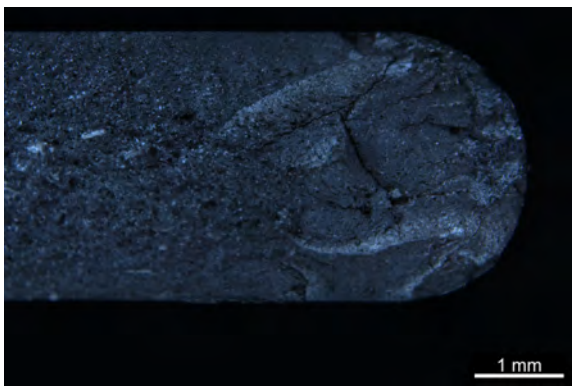

Figure 4.12: DF-F9-2 Defined section

The figures 4.11 and 4.12 show the overview and closeup, respectively, of the fracture surface from the other half of the HPDC reference sample DF-F9. Furthermore, the second peculiar sample in the HPDC reference batch is shown from figure 4.13 to figure 4.16. The connotations "-1" and "-2" represent two halves of the fracture surface. An overview and a closeup of the marked spot is shown for both halves.

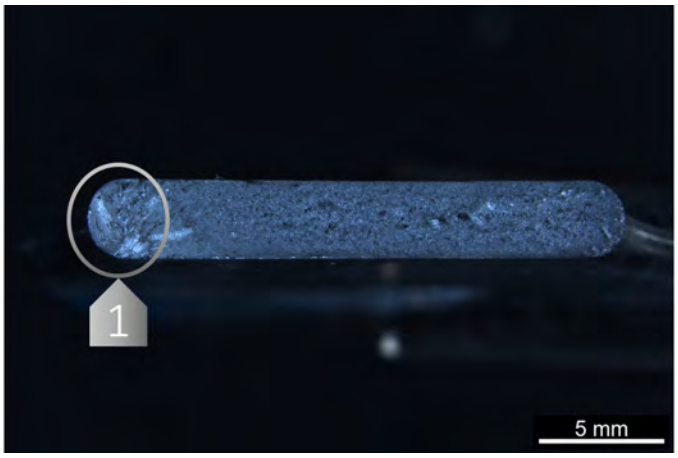

Figure 4.13: DF-F15-1

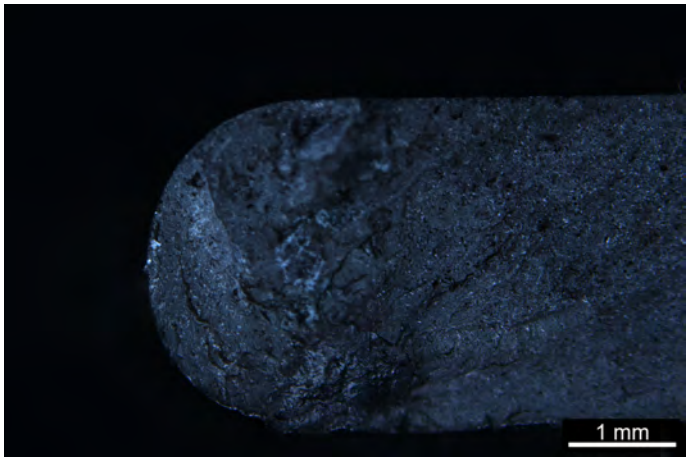

Figure 4.14: DF-F15-1 Defined Section

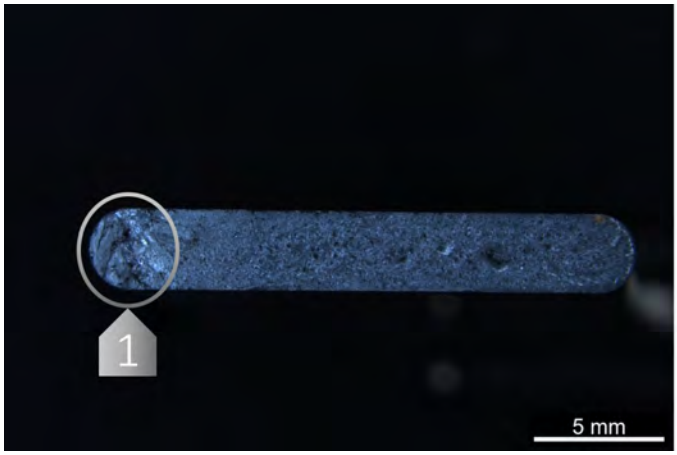

Figure 4.15: DF-F15-2

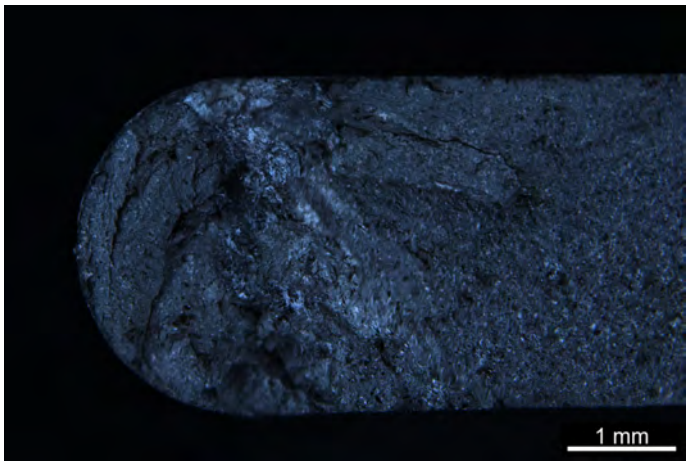

Figure 4.16: DF-F15-2 Defined Section

HPDC anodized samples were tested on the fatigue rig afterward. During the testing, one sample, DF-A-F5 exhibited failure at a low number of cycles and was subsequently examined under a light optical microscope. The microscopic examination aimed to gain insights into the fracture and identify potential factors contributing to the failure. Figure 4.17 shows three sections on the sample that were suspected to have been the cause of failure, whereas figure 4.18 shows the close-up of the sample.

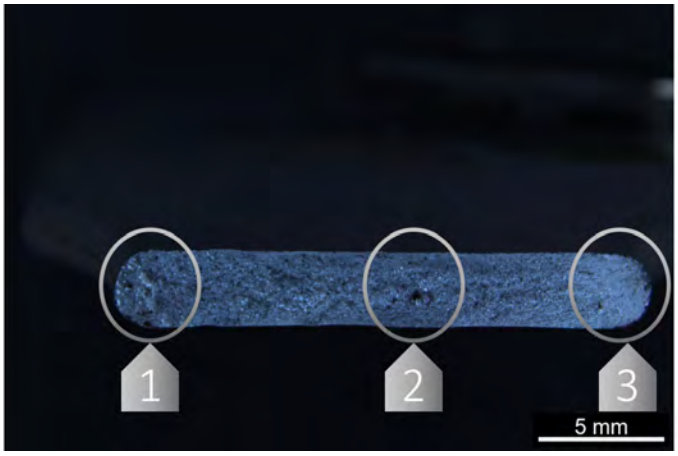

Figure 4.17: DF-A-F5-1

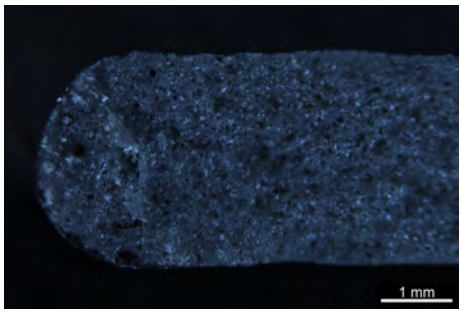

(a) Section 1

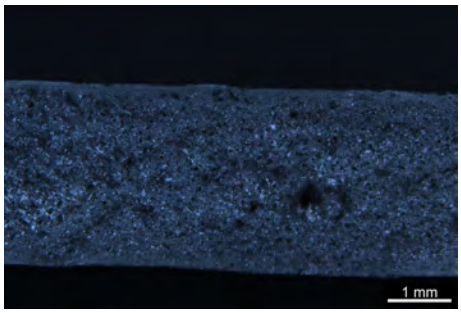

(b) Section 2

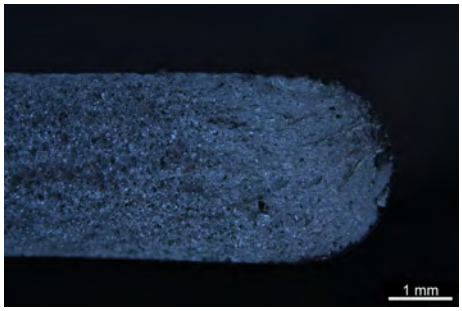

(c) Section 3

Figure 4.18: DF-A-F5-1 Defined section

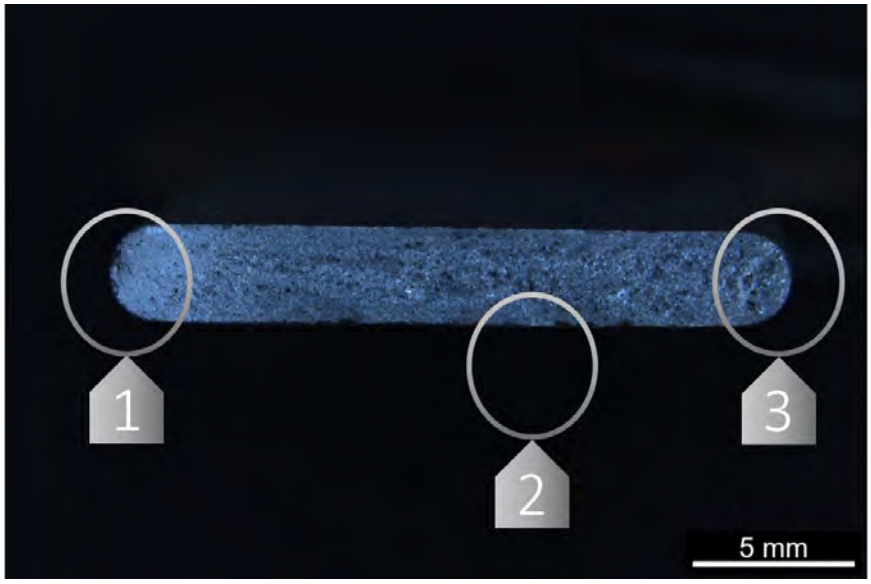

Figure 4.19: DF-A-F5-2

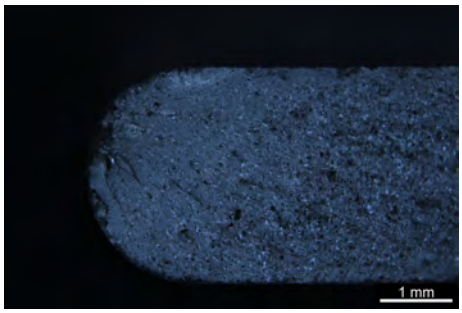

(a) Section 1

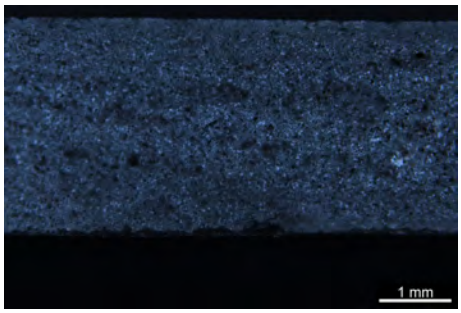

(b) Section 2

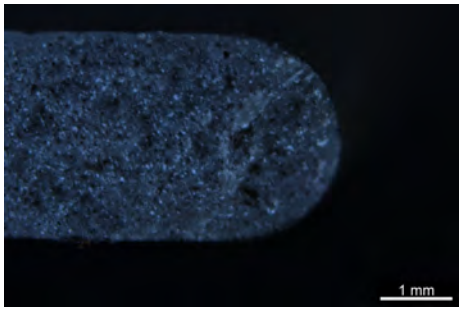

(c) Section 3

Figure 4.20: DF-A-F5-2 Defined section

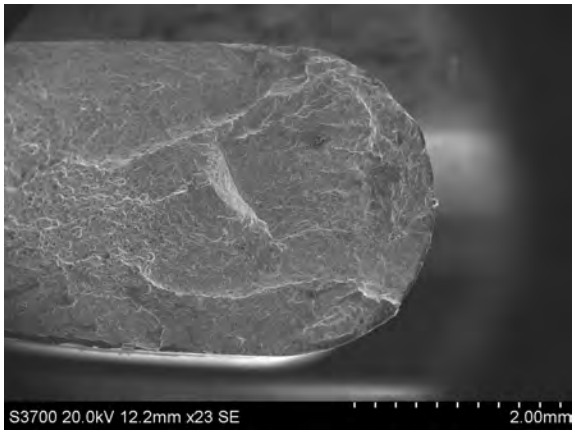

Figure 4.21: DF-F9-2 at section 1 SEM

4.1.4 Scanning Electron Microscopy

4.1.4.1 High Pressure Die Cast

To further understand the peculiar behavior of the alloys, the samples were examined under a scanning electron microscope at Volvo GTT materials technology lab. The results are discussed below.
Similarly, figure 4.22 shows SEM images of an HPDC sample that fractured under 100,000 cycles at very low load settings. In figure 4.22b secondary dendrites can be seen clearly seen inside a shrinkage defect. The large size of these dendrites points to the fact that the melt solidified quickly and there was no time for the micro-

structure to fully develop. Figure 4.22c shows several secondary cracks and oxide layers contributing to the fracture.

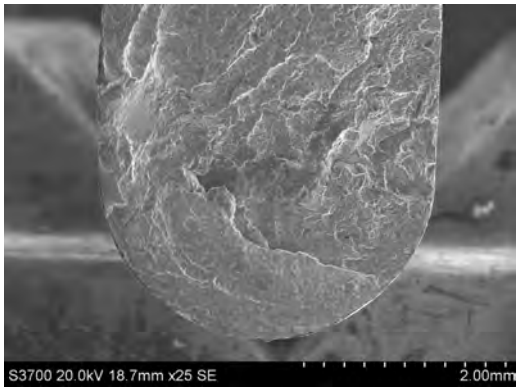

(a) DF-15-2 at section 1 Overview

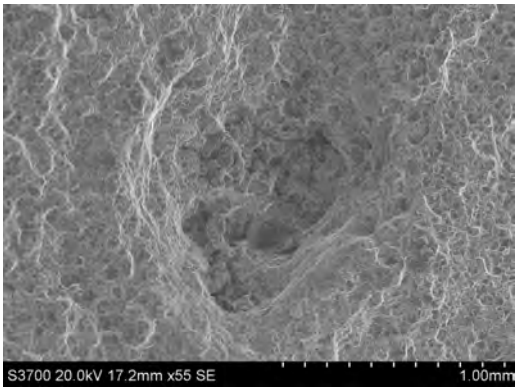

(b) DF-15-2 at section 1-1

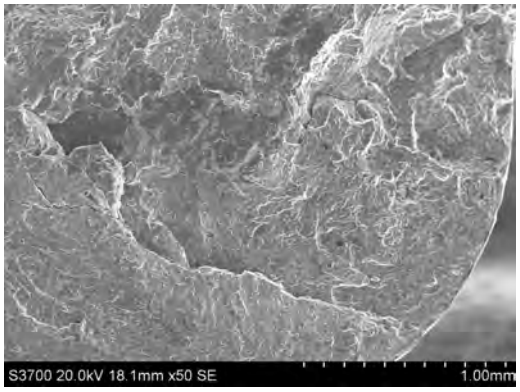

(c) DF-15-2 at section 1-2

Figure 4.22: DF-15-2

4.1.4.2 Permanent Mould Cast

One PMC unanodized sample and two anodized samples were examined under the SEM. The samples "PMC-A-F4" in figure 4.23 and "PMC-A-F5" in figure 4.24 were both tested under the same loading conditions; however, both showed very different fatigue properties. The former achieved almost one million cycles before fracturing, while the latter fractured just above 2,000 cycles.

In the figure 4.23 (a–e), secondary dendrites with traces of intermetallics, crack initiation points, beach marks, secondary cracks, and signs of ductile fracture and shrinkage porosity can be seen. Figure 4.24 shows the SEM images of the other anodized sample, which fractured at relatively low cycles. An even spread of crack initiation sites such as porosities, coarse secondary dendrites, and intermetallics can be seen. Such defects are the major cause of the early fracture of the sample.

Figure 4.25 below shows the SEM image of an unanodized PMC sample that achieved over one and a half million cycles of fracture. Upon examination of the sample, one defect resembling pre-solidification could be seen at a resolution of 100 m. The rest of the material displayed homogeneous material characteristics.

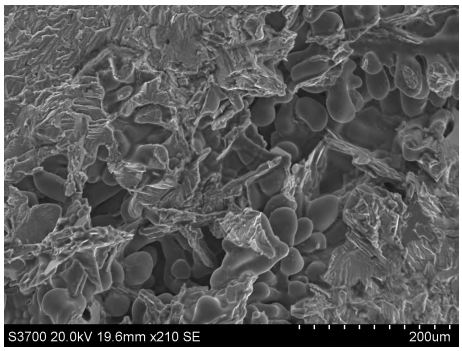

(a) PMC-A-F4-1

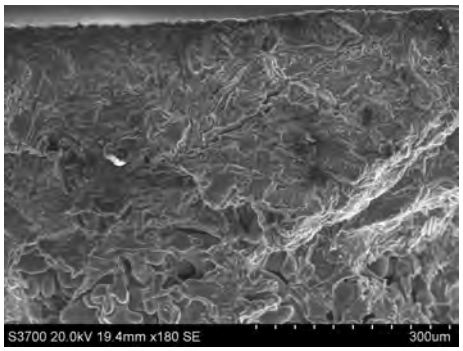

(b) PMC-A-F4-2

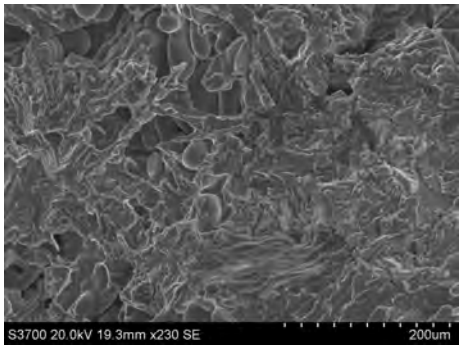

(c) PMC-A-F4-3

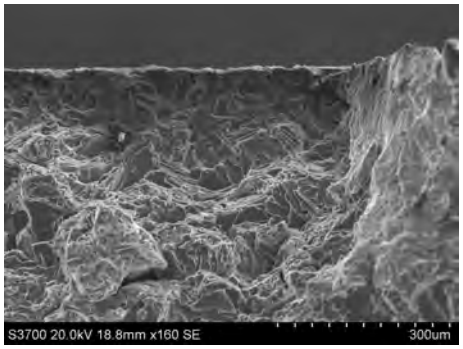

(d) PMC-A-F4-4

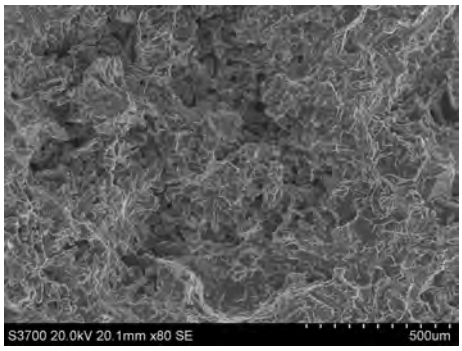

(e) PMC-A-F4-5

Figure 4.23: PMC-A-F4

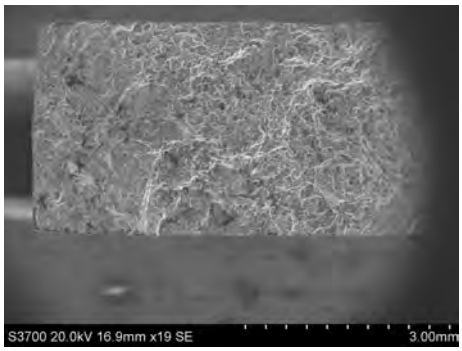

(a) PMC-A-F5-1

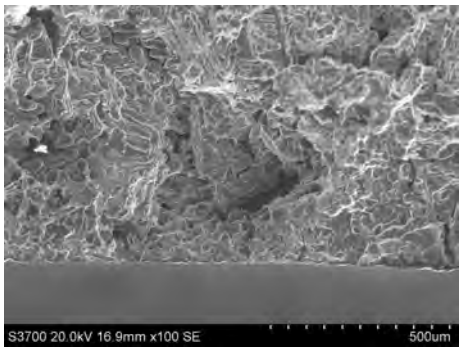

(b) PMC-A-F5-2

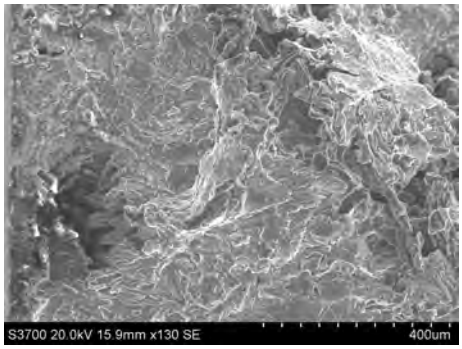

(c) PMC-A-F5-3

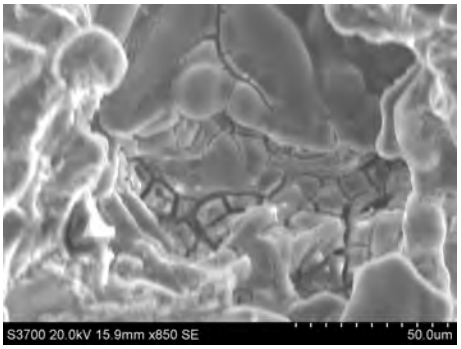

(d) PMC-A-F5-4

Figure 4.24: PMC-A-F5

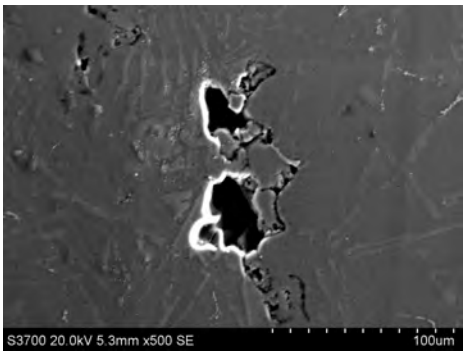

(a) PMC-F7-1

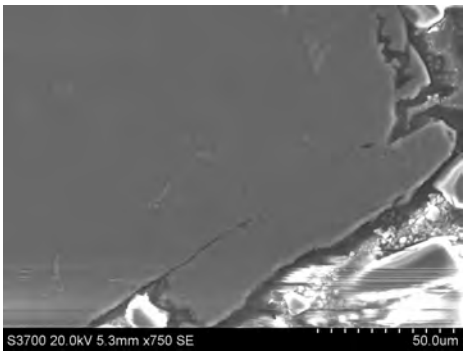

(b) PMC-F7-2

Figure 4.25: PMC-F7

4.1.4.3 Sheet Metal

SEM images of two sheet metal anodized samples namely, "SM-A-F4", figure 4.26 and "SM-A-F6", figure 4.27 are shown below. Clear signs of necking and certain elongation are seen in the figure 4.26b. Material elongates as the cross section reduces before the final fracture. The crack developed from the left-hand side of this image and the final fracture occurred somewhere on the right-hand side of the image. Figure 4.26a shows a high-resolution image of one of the crack initiation cites. The characteristic striations are clearly visible expanding to the left of the image. This implies that the crack initiation point lies somewhere on the right-hand side of the image. A prominent secondary crack is also seen in the same image.

The image shown in figure 4.27 achieved close to the threshold number of cycles to fatigue failure. The nature of the metal made it extremely difficult to detect any anomalies in the microstructure that could have caused the failure, however, at a resolution of 30um distinct striations could be seen.

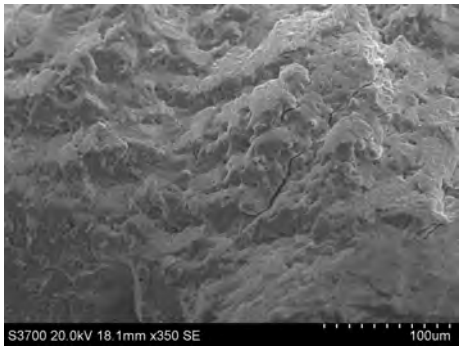

(a) SM-A-F4-1

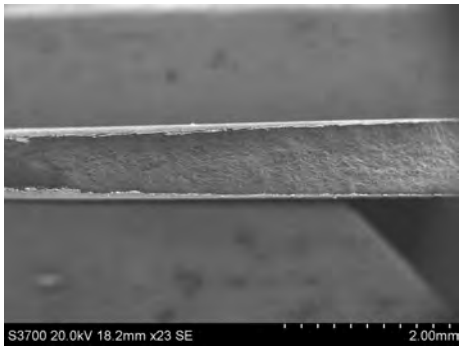

(b) SM-A-F4-2

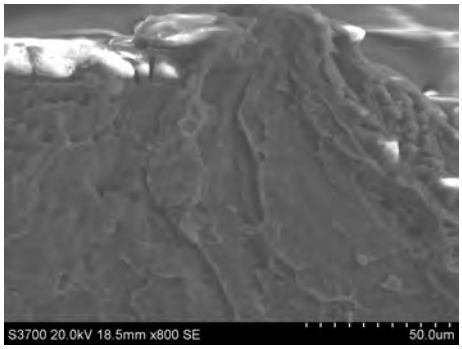

(c) SM-A-F4-3

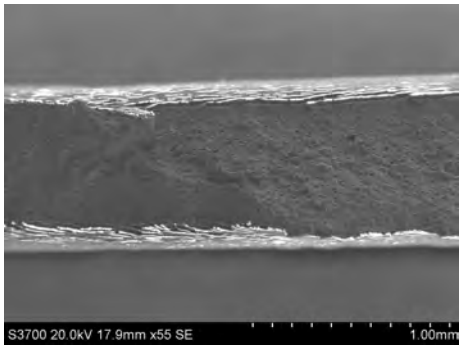

(d) SM-A-F4-4

Figure 4.26: SM-A-F4

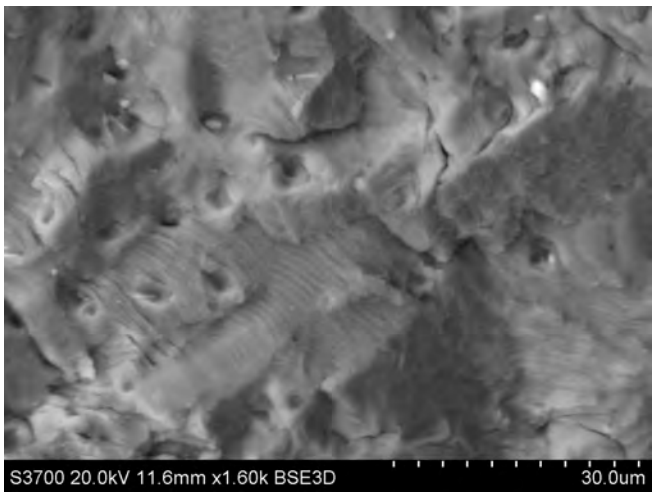

Figure 4.27: SM-A-F6

5
Conclusion

In conclusion, the relationship between fatigue properties and surface treatment of aluminium alloys was studied to shed light on the question of whether or not anodization reduces the fatigue life of aluminium alloys and what were the contributing factors. Three alloys namely 1) High-Pressure Die Cast (EN AC-43400)- HPDC, 2) Permanent Mould Cast (EN AC-43100)- PMC, and 3) Sheet Metal (6014) were acquired from Volvo Penta. The test samples were prepared at both Chalmers University of Technology's prototype lab and Volvo GTT Materials Technology Lab in collaboration with their vendors. The samples were made in dog-bone shapes for fatigue testing. All the fatigue testing was performed at the Department of Material Sciences, Chalmers University of Technology.

The tests were run in material-wise batches, first to set up a reference baseline and then to compare the results for the surface-treated alloys. The data from all the tests were collected and compared for analysis. Various fractography methods were implied on the fractured samples to examine the fracture surfaces and their respective causes of failure. The tests were run with the initial assumption that casting defects would overshadow the detrimental effects of anodization. This assumption held true after conducting a series of tests on HPDC and PMC alloys. Sheet Metal, on the other hand, was tested both after pickling and after anodizing, and the results were compared. The assumption, in this case, was that if pickling is done in a way that does not leave (or leaves a very small quantity of) corrosion pits on the surface, then the follow-up treatment of anodization does not affect the fatigue life.

In summary, the results aligned with initial expectations. Both High-Pressure die-cast and Permanent mould-cast materials exhibited fractures below the chosen threshold (500,000 cycles) due to defects like inclusions, porosities, grain boundaries, and residual stress. This trend was consistent in both reference and anodized samples. Sheet metal tests, conducted in three batches including reference, pickled, and anodized samples, showed that pickled ones displayed superior fatigue properties, attributed to reduced corrosion pits after treatment. Most tests succeeded and had to be manually stopped for new ones. Overall, pickled samples maintained higher fatigue strength, affirming that anodization alone doesn't significantly decrease fatigue strength. An important observation was made during the dye penetrant tests. The test was performed on one unbroken sample for each alloy. All samples had close to 100% defect-free surface solidifying the conclusion that anodization is not the only factor for lower fatigue strength.

The practical knowledge gained during the study is seen as helpful for future material development in the Marine industry for Volvo Penta, and any other industry that might have a use for aluminium alloys, such as the Aerospace/Aviation industries.

Bibliography

[1] Zhu, B. (2017). On the influence of Si on anodising and mechanical properties of cast aluminium alloys (Doctoral dissertation, Jönköping University, School of Engineering).

[2] A.S.T.MD638-10 (2014) Standard Test Method for Tensile Properties of Plastics. ASTM International, West Conshohocken. http://www.astm.org

[3] Rathinam, N., Dhinakaran, R., Sharath, E. (2021). Optimizing process parameters to reduce blowholes in high pressure die casting using Taguchi methodology. Materials Today: Proceedings, 38, 2871-2877.

[4] Zalensas, D. L. (Ed.). (1993). Aluminum casting technology. American Foundrymen's Society.

[5] U.S. Department of Defense. (1993, September 1). MIL-A-8625F: Military Specification Anodizing of Aluminum and Aluminum Alloys. Retrieved from https://everyspec.com/MIL-SPECS/MIL-SPECS-MIL-A/MIL-A-8625F-10769/

[6] U.S. Department of Defense. (1988, April 25). MIL-A-8625E: Military Specification Anodizing of Aluminum and Aluminum Alloys (Superseding MIL-A-8625D). Retrieved from https://assist.dla.mil/quicksearch/basic-profile.cfm?ident-number=6343

[7] Anderson, K., Weritz, J., Kaufman, J. G.(2018). ASM Handbook, Volume 2A: Aluminum Science and Technology. ASM International.

[8] B.Q. Li, Producing Thin Strip by Twin-Roll Casting, Part I: Process Aspects and Quality Issues, J. Met., May 1995, p 29

[9] P. Regan, Recent Advances in Aluminum Strip Casting and Continuous Rolling Technology—Implications for Aluminum Can Body Sheet Production, Light Met. Age, Feb 1992, p 58

[10] Nie, B., Zhang, Z., Zhao, Z., Zhong, Q. (2013). Effect of anodizing treatment on the very high cycle fatigue behavior of 2A12-T4 aluminum alloy. Materials Design, 50, 1005-1010.

[11] Ekaputra, I. M. W., Dewa, R. T., Haryadi, G. D., Kim, S. J. (2020). Fatigue strength analysis of S34MnV steel by accelerated staircase test. Open Engineering, 10(1), 394-400.

[12] Struers. (n.d.). Aluminum - Preparation Methods. Struers Knowledge. Retrieved May 9, 2023, from https://www.struers.com/en/Knowledge/Materials/Aluminumpreparationmethod

[13] Struers. (n.d.). Hot mounting: Achieve the best results in metallography. Retrieved from https://www.struers.com/-/media/Library/Brochures/English/Hot-Mounting.pdf

[14] ASTM, E. 9. (2001). Standard test methods for tension testing of metallic materials. Annual book of ASTM standards. ASTM.

[15] Alteams. (2018). Aluminium Alloy EN-AC 43400 Data Sheet. Retrieved from https://www.alteams.com/content/uploads/2018/11/Aluminium-alloy-EN-AC-43400-data-sheet.pdf

[16] Auto Aluminum Sheet. (n.d.). 6014 Automotive Aluminum Sheet. Retrieved from https://www.autoaluminumsheet.com/product/6014-automotive-aluminum-sheet.html

[17] Murray, M. T., & Murray, M. (2011). High pressure die casting of aluminium and its alloys. In Fundamentals of Aluminium Metallurgy (pp. 217-261). Woodhead Publishing

DEPARTMENT OF INDUSTRIAL AND MATERIALS SCIENCE (IMS)
CHALMERS UNIVERSITY OF TECHNOLOGY
Gothenburg, Sweden
www.chalmers.se

CHALMERS
UNIVERSITY OF TECHNOLOGY